

ROCK: Riesz Occupation kernel methods in RKHSs

Victor Rielly

VICTOR23@PDX.EDU

*Department of Applied Mathematics
Portland State University
Portland, OR 97207*

Kamel Lahouel

KLAHOUEL@TGEN.ORG

Translational Genomics Research Institute, Phoenix, AZ

Chau Nguyen

MIN25@PDX.EDU

*Department of Applied Mathematics
Portland State University
Portland, OR 97207*

Bruno Jedynak

BJEDYNAK2@PDX.EDU

*Department of Applied Mathematics
Portland State University
Portland, OR 97207*

Editor:

Abstract

We present a Representer Theorem result for a large class of weak formulation problems. We provide examples of applications of our formulation both in traditional machine learning and numerical methods as well as in new and emerging techniques. Finally we apply our formulation to generalize the multivariate occupation kernel (MOCK) method for learning dynamical systems from data proposing the more general Riesz Occupation Kernel (ROCK) method. Our generalized methods are both more computationally efficient and performant on most of the benchmarks we test against.

Keywords: RKHS, Occupation kernel, machine learning, dynamical systems, ODEs

1 Introduction

1.1 Proposed contributions

This paper seeks to unite two separate and yet very widely used branches of applied mathematics. On the one hand, numerical methods for PDEs is a very rich branch of mathematics with many rigorous results used throughout engineering practices Alexandre Ern (2004), on the other hand kernel methods for statistical learning is also a well developed and rigorous branch of mathematics Schölkopf and Smola (2002). While numerical methods typically focus on forward problems of solving PDEs, machine learning kernel methods are often used to tackle the inverse problem of learning models from data. We take from both branches of mathematics to present a weak formulation inspired loss that we optimize over Reproducing Kernel Hilbert Spaces. We then demonstrate a handful of examples of applications of our loss among applied mathematics literature. Finally, we apply our loss to

generalize the Occupation Kernel method for learning dynamical systems from data. We present experimental results of our generalized method on real and synthetic data.

1.2 Description of the problem

We present a general framework for many classes of problems, however to provide convincing evidence of the usefulness of the framework we center our experimental results on the concrete task of dynamical system identification. Given data on trajectories $x^1(t), \dots, x^n(t)$ we seek to learn a function $f(x(t))$ characterizing a slopefield from which the trajectories may be predicted with initial conditions. We seek $f(x(t))$ satisfying

$$\dot{x}^i(t) = f(x^i(t)) \quad (1)$$

our proposed method generalizes Rielly et al. (2023) providing a learning algorithm that also scales linearly with d but that often has better performance with much smaller parameter spaces.

1.3 State of the art

We compare with various other models and learning methodologies as described in Rielly et al. (2023) including sparse identification of nonlinear dynamics (SINDy), reduced order models, deep learning methods and latent neural ODEs (Ordinary differential equations). These methods display good performance and are able to scale to problems of thousands of dimensions.

1.4 Related work

Vector Valued Reproducing Kernel Hilbert spaces (vvRKHS) have been gaining a lot of traction in recent years. One work that is very reminiscent of our work may be found in the article Minh et al. (2016) in which they also demonstrate a unified framework of learning in vvRKHSs. This work together with our work points to the power of vvRKHSs to unify seemingly different optimization frameworks. In Minh et al. (2016) the authors do not take a variational approach in the construction of their loss and instead opt to consider a general, convex loss

$$\sum_{i=1}^n V(y_i, Cf(x_i)) \quad (2)$$

where y_i are the data terms, f is the vector valued function to learn, C is a bounded linear operator, and x_i are the inputs to the functions. On the one hand, their loss is more general (V can be any convex loss while we opt to consider the quadratic loss), on the other hand, in their work, they restrict themselves to linear operators applied to f taking the form $Cf(x_i)$ which precludes many linear functionals and bilinear functionals one may encounter in learning problems (for example integrals). In addition, in our framework we are able to relate our loss to a variational problem that allows for the use of test functions. While a representer theorem will work for many choices of losses, a quadratic loss allows for a linear system solution to the optimization problem. For this reason we focus this paper on this simple case.

1.5 More related Work

There is a lot of literature on kernel methods for learning and solving PDEs and dynamical systems using collocation points. In particular, our intuition closely resembles the intuition in optimal recovery. For example, in Owhadi and Scovel (2019) the central problem proposed in chapter 3 for optimal recovery splines in 3.7 also solves an infimum of a supremum. In our case we take a supremum over functions of norm 1 while in Owhadi and Scovel (2019) the authors minimize the ratio of a loss and the norm of the function which for the case of linear Ψ (see Owhadi and Scovel (2019) equation 3.7), is equivalent to our formulation. One important distinction between the loss we propose and the loss presented in Owhadi and Scovel (2019) is our loss uses linear functionals and bilinear functionals to send all terms to real valued constants while the loss for optimal recovery computes the norm of the residual in the space of candidate functions. Nevertheless, in both cases an analytic expression for a solution is provided (See chapter 3 theorem 3.1 of Owhadi and Scovel (2019)). Further work along these lines may be found in Long et al. (2023). There are many similarities with our work and the work in Long et al. (2023) and Owhadi and Scovel (2019). However, we focus our analysis on dynamical systems while these works focus on partial differential equations. We make use of a weak formulation with test functions to define our “measurements” (to borrow from the language in Owhadi and Scovel (2019)). In addition we present our results in the context of vvRKHSs which allows us to take advantage of the computational benefits of using a separable kernel as described in Rielly et al. (2023). Finally, although many extensions to nonlinear problems arise naturally from our framework, we focus on the linear problem as it is both very general and provides a good introduction to the ideas and techniques.

2 Background and Notation

2.1 Notation

In the following list, we provide some of the common notation standards we use throughout this paper.

1. \mathbb{R} denotes the real line, all other boldface capital characters, for example \mathbb{H} , will denote Hilbert Spaces.
2. $K_{\mathbb{H}}(\cdot, *)$ denotes the matrix valued kernel function for the vector valued Reproducing Kernel Hilbert Space (vvRKHS) \mathbb{H}
3. $k(\cdot, *)$ or $k_{\mathbb{H}}(\cdot, *)$ will be used to denote a scalar valued kernel for a Reproducing Kernel Hilbert space (RKHS) \mathbb{H} . Scalar valued RKHSs are vector valued RKHSs for which the matrix valued kernel is 1×1 (scalar valued).
4. Let \mathcal{X} denote a nonempty set of elements.
5. $M_{i,j;l,m}$ denotes the i, j th row, and the l, m th column of matrix M . Double indexing is sometimes required. To remain consistent, entries of multi-indexed matrices (and vectors) will always have the same indexing scheme. This scheme will have entries of M sorted first by the first index, then the second then so on.

6. e_j denotes the 0,1 vector in \mathbb{R}^d for which only the j th entry is 1.

2.2 Reproducing Kernel Hilbert Spaces

Our methodology makes heavy use of vector valued Reproducing Kernel Hilbert Spaces. For a thorough reference see Paulsen and Raghupathi (2016).

Definition 1 *Let \mathbb{H} be a Hilbert space of vector valued functions taking a nonempty set \mathcal{X} to \mathbb{R}^d . We call \mathbb{H} a vector valued RKHS (vvRKHS) if for every $v \in \mathbb{R}^d$, and $x \in \mathcal{X}$, the linear functional*

$$l_{v,x}(f) \equiv f(x)^T v \quad (3)$$

is bounded.

If \mathbb{H} is a vvRKHS we may observe the following.

1. For every $l_{v,x}$ Riesz representation theorem guarantees the existence of a unique $l_{v,x}^* \in \mathbb{H}$ for which

$$l_{v,x}(f) = f(x)^T v = \langle f, l_{v,x}^* \rangle_{\mathbb{H}} \quad (4)$$

Observe that for any $v, w \in \mathbb{R}^d$ and $x, y \in \mathcal{X}$

$$l_{v,x}(l_{w,y}^*) = l_{w,y}^*(x)^T v \quad (5)$$

$$= \langle l_{w,y}^*, l_{v,x}^* \rangle_{\mathbb{H}} \quad (6)$$

$$= \langle l_{v,x}^*, l_{w,y}^* \rangle_{\mathbb{H}} \quad (7)$$

$$= l_{w,y}(l_{v,x}^*) \quad (8)$$

$$= l_{v,x}^*(y)^T w \quad (9)$$

Thus $l_{v,x}(l_{w,y}^*)$ is a bilinear functional of v and w . It can therefor be written in the form

$$v^T K(x, y) w \quad (10)$$

for some matrix valued $K(x, y)$. This in turn implies

$$l_{v,x}^*(y)^T w = v^T K(x, y) w \Rightarrow l_{v,x}^*(y)^T = v^T K(x, y) \quad (11)$$

and similarly

$$l_{w,y}^*(x)^T = w^T K^T(x, y) \quad (12)$$

but since we chose w, v, y, x arbitrarily we also have (after substituting w for v and y for x)

$$l_{w,y}^*(x)^T = w^T K(y, x) \quad (13)$$

Thus

$$K^T(x, y) = K(y, x) \quad (14)$$

Using $v = e_i$ and $w = e_j$ we can define $K(x, y)$ by

$$e_i^T K(x, y) e_j = l_{e_i, x}(l_{e_j}^*(y)) = l_{e_j, y}(l_{e_i}^*(x)) = K(x, y)_{i,j} \quad (15)$$

2. The kernel function $K(x, y)$ is positive semidefinite. In other words, for any $x_1, \dots, x_n \in \mathcal{X}$, $\alpha_1, \dots, \alpha_n \in \mathbb{R}^d$,

$$\sum_{i=1}^n \sum_{j=1}^n \alpha_i^T K(x_i, x_j) \alpha_j \geq 0 \quad (16)$$

To see this observe:

$$\sum_{i=1}^n \sum_{j=1}^n \alpha_i^T K(x_i, x_j) \alpha_j = \sum_{i=1}^n \sum_{j=1}^n \langle l_{x_i, \alpha_i}^*, l_{x_j, \alpha_j}^* \rangle \quad (17)$$

$$= \left\langle \sum_{i=1}^n l_{x_i, \alpha_i}^*, \sum_{j=1}^n l_{x_j, \alpha_j}^* \right\rangle \quad (18)$$

$$= \left\| \sum_{i=1}^n l_{x_i, \alpha_i}^* \right\|_{\mathbb{H}}^2 \geq 0 \quad (19)$$

3. We also have the reproducing property. Recalling

$$l_{v,x}^*(y)^T = v^T K(x, y) \Rightarrow l_{v,x}^*(y) = K^T(x, y)v = K(y, x)v \quad (20)$$

we have

$$f(x)^T v = \langle f, l_{v,x}^*(\cdot) \rangle = \langle f, K(\cdot, x)v \rangle \quad (21)$$

All finite dimensional Hilbert spaces are equivalent (in the sense that their norms are equivalent). Therefore, all finite dimensional Hilbert spaces of functions are reproducing kernel Hilbert spaces. Here we demonstrate how to construct a kernel for any Hilbert space of vector valued functions. This very simple known result is very useful so is provided below for completeness.

Proposition 2 *Let \mathbb{H} be a Hilbert space of vector valued functions where for each $f, g \in \mathbb{H}$, $f(x) \in \mathbb{R}^d$ takes $x \in \mathcal{X}$ to \mathbb{R}^d with real valued inner product $\langle f, g \rangle_{\mathbb{H}} \in \mathbb{R}$. And let $\{b_1(x), \dots, b_n(x)\}$ be an orthonormal basis for this Hilbert space of functions. Then \mathbb{H} is a vector valued RKHS with kernel function*

$$K_{\mathbb{H}}(x, y) = \Psi(x)^T \Psi(y) \quad (22)$$

where

$$\Psi(x) = \begin{bmatrix} b_1(x)^T \\ \vdots \\ b_n(x)^T \end{bmatrix} \quad (23)$$

3 Existence and uniqueness

We present an existence and uniqueness result for a general variational problem where the test functions arise from a finite dimensional vector valued reproducing kernel Hilbert space while the solution functions arise from a general vector valued reproducing kernel Hilbert.

Proposition 3 (Riesz Representation) *Let \mathbb{H} be a vector valued RKHS taking a set \mathcal{X} to \mathbb{R}^d , and l be a **bounded** linear functional taking \mathbb{H} to \mathbb{R} then there is a unique $l^* \in \mathbb{H}$ for which for any $h \in \mathbb{H}$*

$$l(h) = \langle h, l^* \rangle_{\mathbb{H}}$$

Where $\langle \cdot, * \rangle_{\mathbb{H}}$ is the inner product in \mathbb{H} . Moreover l^* is given by

$$l^*(x) = \sum_{i=1}^d l(K_{\mathbb{H}}(\cdot, x)e_i) e_i$$

Where $K_{\mathbb{H}}(\cdot, *)$ is the reproducing kernel for the RKHS.

For a proof see the supplementary material.

Theorem 4 (Existence and Uniqueness) *Let $\mathbb{H}, \mathbb{V}_1, \dots, \mathbb{V}_n$ be vector valued RKHSs with kernels $K_{\mathbb{H}}, K_{\mathbb{V}_1}, \dots, K_{\mathbb{V}_n}$, inner products $\langle \cdot, * \rangle_{\mathbb{H}}, \langle \cdot, * \rangle_{\mathbb{V}_1}, \dots, \langle \cdot, * \rangle_{\mathbb{V}_n}$ and norms $\|\cdot\|_{\mathbb{H}}, \|\cdot\|_{\mathbb{V}_1}, \dots, \|\cdot\|_{\mathbb{V}_n}$ respectively. Assume \mathbb{H} takes a set \mathcal{X} to \mathbb{R}^d and \mathbb{V}_i takes a set \mathcal{Y}_i to \mathbb{R}^{d_i} . Assume also $\mathbb{V}_1, \dots, \mathbb{V}_n$ are finite dimensional with dimensions q_1, \dots, q_n and feature functions Ψ_1, \dots, Ψ_n with $\Psi_i : \mathcal{Y}_i \Rightarrow \mathbb{R}^{q_i \times d_i}$ respectively. Let p_1, \dots, p_n be bilinear functionals taking $\mathbb{H} \times \mathbb{V}_i$ to \mathbb{R} that are continuous with respect to both entries. That is to say, for a fixed $v \in \mathbb{V}_i$, There is a constant K_v such that for any $h \in \mathbb{H}$.*

$$|p_i(h, v)| \leq K_v \|h\|_{\mathbb{H}} \quad (24)$$

and for any fixed $h \in \mathbb{H}$ there is a constant K_h such that for any $v \in \mathbb{V}_i$

$$|p_i(h, v)| \leq K_h \|v\|_{\mathbb{V}_i} \quad (25)$$

Let l_1, \dots, l_n be continuous linear functionals taking $\mathbb{V}_1, \dots, \mathbb{V}_n$ to \mathbb{R} so that there is a constant K_i such that for any $v \in \mathbb{V}_i$,

$$|l_i(v)| \leq K_i \|v\|_{\mathbb{V}_i} \quad (26)$$

(Note, since \mathbb{V}_i are finite dimensional, all linear functionals taking \mathbb{V}_i to \mathbb{R} are bounded) then for any strictly increasing function $\lambda : [0, \infty) \rightarrow [0, \infty)$ there is a unique solution to the variational problem:

$$\inf_{f \in \mathbb{H}} \left\{ \sum_{i=1}^n \sup_{\{v \in \mathbb{V}_i \mid \|v\|=1\}} \left\{ (p_i(f, v) - l_i(v))^2 \right\} + \lambda(\|f\|_{\mathbb{H}}^2) \right\} \quad (27)$$

Moreover, assuming $\lambda(\|x\|_{\mathbb{H}}^2) = \lambda \cdot \|x\|_{\mathbb{H}}^2, \lambda > 0$ (is the quadratic function) this unique solution is given by solving the linear system

$$(M + \lambda I) \alpha = y \quad (28)$$

with $\forall x \in \mathcal{X}$, $f(x)$ given by

$$f(x) = \sum_{i=1}^n \sum_{k=1}^{q_i} \alpha_{i,k} \mathcal{L}_{i,k}^*(x) \quad (29)$$

where

$$\mathcal{L}_{i,k}^*(*) = \sum_{j=1}^d p_i(K_{\mathbb{H}}(\cdot, *)e_j, \Psi_i(\cdot)^T e_k)e_j \quad (30)$$

Letting $N = \sum_{i=1}^n q_i$, $M \in \mathbb{R}^{N \times N}$ is given by

$$M_{l,m:i,k} = \langle \mathcal{L}_{l,m}^*, \mathcal{L}_{i,k}^* \rangle_{\mathbb{H}} \quad (31)$$

so that

$$M = \begin{bmatrix} M_{1,1} & \dots & M_{1,n} \\ \vdots & \ddots & \vdots \\ M_{n,1} & \dots & M_{n,n} \end{bmatrix}$$

where the i, j th block is the matrix:

$$M_{i:j} = \begin{bmatrix} M_{i,1:j,1} & \dots & M_{i,1:j,q_j} \\ \vdots & \ddots & \vdots \\ M_{i,q_i:j,1} & \dots & M_{i,q_i:j,q_j} \end{bmatrix}$$

with

$$M_{l,m:i,k} = \langle \mathcal{L}_{l,m}^*, \mathcal{L}_{i,k}^* \rangle_{\mathbb{H}} = p_i \left(\sum_{j=1}^d p_l(K_{\mathbb{H}}(\cdot, *)e_j, \Psi_l(\cdot)^T e_m) e_j, \Psi_i(*)^T e_k \right) \quad (32)$$

and y is given by

$$y_{i,k} = l_i(\Psi_i(\cdot)^T e_k) \quad (33)$$

so that

$$y^T = [y_{1,1}, \dots, y_{1,q_1}, y_{2,1}, \dots, y_{2,q_2}, \dots, y_{n,q_n}] \quad (34)$$

The proof is provided in the supplementary material.

4 Example applications

In the following subsections we demonstrate a collection of optimization problems that all fall within this framework. In the case of the MOCK example, we provide the derivation of the optimal solution using 7 to compare with the results of Rielly et al. (2023).

4.1 Multivariate Regression

Consider the task of learning a vector valued function given samples $x_1, \dots, x_n \in \mathcal{X}$ and (perhaps noisy) samples of the evaluation of the unknown function $y_1, \dots, y_n \in \mathbb{R}^p$. This is often done by minimizing the following regression loss

$$\inf_{f \in \mathbb{H}} \left\{ \sum_{i=1}^n \|f(x_i) - y_i\|_{\mathbb{R}^p}^2 + \lambda \|f\|_{\mathbb{H}}^2 \right\} \quad (35)$$

We may rewrite this loss as follows:

$$\inf_{f \in \mathbb{H}} \left\{ \sum_{i=1}^n \sum_{j=1}^p (f(x_i)^T e_j - y_i^T e_j)^2 + \lambda \|f\|_{\mathbb{H}}^2 \right\} \quad (36)$$

Consider the somewhat trivial one dimensional space of constant test functions:

$$V_{i,j}(x) = \text{span}\{e_j\} \quad (37)$$

together with the inner product $\langle \alpha e_j, \beta e_j \rangle = \alpha \beta$. This is an RKHS as it is a one dimensional Hilbert space of constant functions into \mathbb{R}^p . 2 tells us the feature transformation for this function is

$$\Psi(\cdot) = e_j^T \quad (38)$$

and the kernel is the constant matrix

$$K(\cdot, *) = e_j e_j^T \quad (39)$$

Since the subset of $V_{i,j}$ containing all functions of norm 1, is a set containing the two elements e_j and $-e_j$, we may trivially transform the problem into:

$$\inf_{f \in \mathbb{H}} \left\{ \sum_{i=1}^n \sum_{j=1}^p \sup_{\{v \in V_{i,j} \mid \|v\|=1\}} \left\{ (f(x_i)^T v(x_i) - y_i^T v(x_i))^2 \right\} + \lambda (\|f\|_{\mathbb{H}}^2) \right\} \quad (40)$$

Here we adopt the somewhat unusual notation of writing constant functions e_j as $v(x_i)$ functions of x_i . And indeed it is also convenient to think of $y_i = y(x_i)$ as well. For any fixed $v \in V_{i,j}$,

$$p_{i,j}(f, v) = f(x_i)^T v(x_i) \quad (41)$$

is a continuous linear functional of f as \mathbb{H} is a vector valued RKHS. Thus, for any vvRKHS \mathbb{H} , traditional multivariate regression is an example application of 7. One can check directly that the solution provided by 7 is the same as the standard ridge regression solution (see the supplementary material).

4.2 Finite Elements Analogy

Engineers that solve partial differential equations (PDEs) to model physical systems often make use of finite elements methods and galerkin methods. These methods consider an abstract linear problem which serves as a generic model for such engineering applications. In chapter 2 of Alexandre Ern (2004) this generic problem is considered along with conditions under which this problem is well-posed.

$$\left\{ \begin{array}{ll} \text{Seek } u \in W & \text{such that} \\ a(u, v) = f(v), & \forall v \in V \end{array} \right. \quad (42)$$

Although the theory for this problem is proven for Banach spaces W and V , in practical applications, such as whenever engineers solve PDEs, the spaces W and V are usually taken

to be Hilbert spaces such as Sobolev spaces. a is a continuous bilinear form taking $W \times V$ to \mathbb{R} and f is a continuous linear form on V taking V to \mathbb{R} .

However, this problem is not always well posed. Sometimes there are no solutions, sometimes many solutions. Indeed, one way to see this is to consider the linear algebra analogue to the problem: Let A be a matrix. Let W, V be spaces of vectors, and $u \in W$ and $v, f \in V$. Consider the analogous problem

$$\begin{cases} \text{Seek } u \in W & \text{such that} \\ v^T A u = v^T f, & \forall v \in V \end{cases} \quad (43)$$

If the matrix A is not invertible, there may be no solution to the problem or many solutions.

Finite Elements methods deal with the case where V and W are the same space, while Galerkin methods deal with the case where V is not W . The traditional numerical approach is to begin by guaranteeing that the problem is well posed using coercivity of the bilinear operator a and Lax-Milgram (or its extension to the case where V is not W Banach-Necas-Babuska)(see Chapter 2 Alexandre Ern (2004)). This would be analogous to determining that the matrix A in the linear system is invertible. Then, numerical methods seek to solve the linear system. Our approach instead is more similar to a least-squares regression approach. If a solution to the problem (42)

exists, it will satisfy

$$\sup_{\{v \in V \mid \|v\|=1\}} \{(a(u, v) - f(v))^2\} = 0 \quad (44)$$

moreover, if we find $u \in W$ such that

$$\sup_{v \in V \mid \|v\|=1} \{(a(u, v) - f(v))^2\} = 0 \quad (45)$$

and V is sufficiently expressive, then this will be a solution to the problem (42) However, even if a solution to this problem does not exist, we can still find a solution to

$$\inf_{u \in W} \left\{ \sup_{v \in V \mid \|v\|=1} \{(a(u, v) - f(v))^2\} \right\} \quad (46)$$

Moreover, if multiple solutions exist, we will find a minimum norm solution in W . In this way we are able to proceed without requiring coercivity of the bilinear form. In addition, we are still sometimes able to provide a posteriori error results for solutions of our formulation (much like can be done for using least squares regression to estimate the solution to a linear system). For the case where W and V are vvRKHS (for example, infinite-dimensional or smooth enough Sobolev spaces) we can always provide a solution to this problem.

Moreover, our initial analysis indicates that the regularization term is critical in ensuring the best convergence even in the no-noise numerical case as the quality of convergence is often dependent on the regularity of the final solution.

4.3 Learning PDEs example

Let $v \in \mathbb{H}$ where \mathbb{H} is a vector valued RKHS that takes x , and u and sends it to \mathbb{R} and let $P(v, x, u)$ be some vector valued differential operator of the function v . Assume the PDE

solution $u(x) \in \mathcal{B}$ belongs to a Banach space. Assume the differential operator P is linear in v . Then we can solve an inverse problem, that is learn v given data on u , satisfying

$$P(v, x, u(x)) = f(x, u(x), D(u(x))) \quad (47)$$

by minimizing the loss

$$\inf_{v \in \mathbb{H}} \left\{ \sup_{\{\tau \in \mathbb{V}, \|\tau\|=1\}} \left\{ \left(\int_{\Omega} (P(v(x, u), x, u) - f(x, u, D(u)))^T \tau(x) dx \right)^2 \right\} + \lambda (\|v\|_{\mathbb{H}}^2) \right\} \quad (48)$$

Here, $D(u(x))$ may be some differential operator of u and f a function of x, u and $D(u)$. \mathbb{V} can be chosen to be a finite dimensional vector valued RKHS. Here we see

$$\int_{\Omega} P(v(x, u(x)), x, u(x))^T \tau(x) dx \quad (49)$$

is a bilinear form of v and τ and

$$\int_{\Omega} f(x, u(x), D(u))^T \tau(x) dx \quad (50)$$

is a linear functional of τ . If we can show these are bounded, we may apply 7 to arrive at the solution.

As a practical example, consider the Schrodinger equation:

$$i\hbar \frac{\partial \Psi(t, x)}{\partial t} = \frac{-\hbar^2}{2m} \frac{\partial^2 \Psi(t, x)}{\partial x^2} + V(t, x) \Psi(t, x) \quad (51)$$

if we are given enough measurements of the wavefunction, we may in principle learn the potential function V with a variational approach by solving a linear system. Conversely, if we are given the potential function V we can solve for the wave function as the differential equation is linear in the wave function. If however we are not given sufficient data on either, we may still desire to predict the potential function while simultaneously predicting the wavefunction to match what little data we do have. This task would be a nonlinear optimization problem as the PDE is quadratic in the combination of the wavefunction and the potential function.

As a concrete demonstration of a learning problem implementation, consider the problem of learning $\alpha(x), f(u(x, y))$ for the quasilinear PDE

$$\alpha(x)u_x(x, y) + u_y(x, y) = f(u(x, y)) \quad (52)$$

given samples of $u(x, y)$ on a uniform grid for the domain $(x, y) \in [-4, 4] \times [0, 1]$. To solve this inverse problem, we will minimize

$$\inf_{f \in \mathbb{H}_1, \alpha \in \mathbb{H}_2} \left\{ \sup_{\{v \in \mathbb{V}, \|v\|=1\}} \left\{ \int_0^1 \int_{-4}^4 (\alpha(x)u_x(x, y) + u_y(x, y) - f(u(x, y))) v(x, y) dx dy \right\} \right\} \quad (53)$$

on the domain $(x, y) \in [-4, 4] \times [0, 1]$. For this problem, and for $u(x, y)$ given by

$$u(x, y) = \left(1 + e^{y + \sin(4\pi(\arctan(x) - y))}\right)^{-1} \quad (54)$$

One can check directly that $u(x, y)$ satisfies

$$(1 + x^2)u_x(x, y) + u_y(x, y) = u(x, y)(u(x, y) - 1) \quad (55)$$

Here, all RKHSs are scalar valued and the infimum is taken over two RKHSs. However, defining a new RKHS with kernel $K_{\mathbb{H}}(\cdot, *) \in \mathbb{R}^{2 \times 2}$ with $K_{\mathbb{H}}(\cdot, *)_{1,1} = k_{\mathbb{H}_1}(\cdot, *)$ and $K_{\mathbb{H}}(\cdot, *)_{2,2} = k_{\mathbb{H}_2}(\cdot, *)$ and $K_{\mathbb{H}}(\cdot, *)_{1,2} = K_{\mathbb{H}}(\cdot, *)_{2,1} = 0$ easily converts the problem into one of the form described by 7. We provide detailed derivations of the methodology in the supplementary materials.

For our experiments, we sample $u(x, y)$ on a uniform grid over the domain. We take n samples evenly from -4 to 4 for the x values (n ranging from 100 to 12800) and for each of these, we take m samples evenly from 0 to 1 across the y axis (m ranging from 10 to 1280). Thus we have anywhere from 1000 to 16.384 million samples. We estimate α and f by minimizing 48 using only our samples of u , and integrating with a trapezoid rule quadrature. 11 demonstrates our error in the recovered functions α and f in terms of the number of samples of u . This error is reported as

$$\frac{\text{mean}(|\alpha(x_i) - \hat{\alpha}(x_i)|)}{\text{mean}(|\alpha(x_i)|)} \cdot 100\%$$

and

$$\frac{\text{mean}(|f(x_i, y_j) - \hat{f}(x_i, y_j)|)}{\text{mean}(|f(x_i, y_j)|)} \cdot 100\%.$$

One thing to note is we assume an explicit (parametric) form for α and f with 100 parameters each for α and f . Thus our linear systems are 200 dimensional for all experiments. This is in contrast to finite elements methods for which the linear systems typically scale linearly with the number of locations to estimate the solution. Nevertheless we see continuing improvements in the loss as we increase the sample count. We are not able to saturate the expressiveness of the solution space even with over 16 million samples. This indicates we may benefit from using higher order quadratures to observe quicker convergence rates. 1 provides some visualizations of the PDE and the solution.

We provide this problem as an example as learning PDE's is a relatively new and emerging field in machine learning and mathematics, see Raissi et al. (2019), Gao et al. (2022), Boullé et al. (2022), Stephany and Earls (2024). This variational framework allows engineers to naturally construct a loss to handle these types of inverse problems even in the case where the PDE is non-linear so long as it depends linearly on the unknown and learned functions. The empirical convergence rates are also what one might expect from numerical results for solving variational problems in finite elements and Galerkin methods hinting at directions for convergence gaurantees.

n	m	α -error	f -error
100	10	21%	29%
200	20	4%	3.5%
400	40	.9%	.8%
800	80	.2%	.2%
1600	160	.06%	.05%
3200	320	.01%	.01%
6400	640	.003%	.003%
12800	1280	.0009%	.0008%

Table 1: Estimation errors for α and f (reported as percent error of α and f measured on the grid points). Although we fix the number of Fourier random features to 100 for alpha and 100 for f in all experiments, we see the error still decreases in proportion to the inverse of nm (the total number of samples) as n , and m increase. Where n is the number of samples taken across x and m is the number of samples across y in the grid. This suggests that errors may be improved with more data even as we fix the size of the solution space. This is in contrast to finite element methods which typically see the solution space grow with the number of samples. It also suggests we may see faster convergence if we use a higher order quadrature in the integration. For this demonstration we simply stick to the trapezoid rule to compute our integrals.

4.4 MOCK

Consider the problem of learning a function $f : \mathbb{R}^d \rightarrow \mathbb{R}^d$ satisfying

$$\dot{x}^i(t) = f(x^i(t)) \quad (56)$$

from snapshots of trajectories (as presented in Rielly et al. (2023)). Where we have n trajectories, $x^1(t), \dots, x^n(t) \in \mathbb{R}^d$, and for each $i \in 1, \dots, n$ there are n_i samples $x_j^i = x^i(t_j^i)$ of the trajectories. As in Rielly et al. (2023) we may consider minimizing the loss:

$$\min_{f \in \mathbb{H}} \left\{ \sum_{i=1}^n \sum_{j=1}^{n_i-1} \left\| \int_{t_j^i}^{t_{j+1}^i} (f(x^i(t)) - \dot{x}^i(t)) dt \right\|^2 + \lambda \|f\|_{\mathbb{H}}^2 \right\} \quad (57)$$

Rearranging the terms, it is easy to see this loss is of the correct form for 7. Indeed, letting $\mathbb{V}_{i,j,k}$ be the one dimensional space of constant functions (that are nonzero only in one coordinate) in \mathbb{R}^d for which $\|e_k\|_{\mathbb{V}_{i,j,k}} = 1$.

$$\mathbb{V}_{i,j,k} = \text{span}\{e_k\}$$

and rewriting the \mathbb{R}^d norm as a sum gives us the loss:

$$\min_{f \in \mathbb{H}} \left\{ \sum_{i=1}^n \sum_{j=1}^{n_i-1} \sum_{k=1}^d \left(\int_{t_j^i}^{t_{j+1}^i} (f(x^i(t)) - \dot{x}^i(t)) e_k dt \right)^2 + \lambda \|f\|_{\mathbb{H}}^2 \right\} \quad (58)$$

Since $\mathbb{V}_{i,j,k}$ is a one dimensional space the subset of all functions of norm 1 of $\mathbb{V}_{i,j,k}$ is a set containing just the two $e_k, -e_k$ vectors. So we may replace the loss with:

$$\min_{f \in \mathbb{H}} \left\{ \sum_{i=1}^n \sum_{j=1}^{n_i-1} \sum_{k=1}^d \sup_{\{v \in \mathbb{V}_{i,j,k}, \|v\|=1\}} \left\{ \left(\int_{t_j^i}^{t_{j+1}^i} f(x^i(t))^T v(t) dt - \int_{t_j^i}^{t_{j+1}^i} \dot{x}^i(t)^T v(t) dt \right)^2 \right\} + \lambda \|f\|_{\mathbb{H}}^2 \right\} \quad (59)$$

Since $\mathbb{V}_{i,j,k}$ is 1 dimensional and the operators are linear, they are bounded. All that remains to show is that

$$\int_{t_j^i}^{t_{j+1}^i} f(x^i(t))^T v(t) dt \quad (60)$$

is a bounded linear functional with respect to f . For this, let's assume $v(t)$ is fixed and finitely integrable (indeed it is a constant finite function for MOCK). For any interval of integration $[a, b]$ and any trajectory $x(t)$ boundedness of this linear functional requires:

$$\left| \int_a^b f(x(t))^T v(t) dt \right| \leq \int_a^b |f(x(t))^T v(t)| dt \quad (61)$$

$$= \int_a^b |\langle f, K_{\mathbb{H}}(\cdot, x(t))v(t) \rangle| dt \quad (62)$$

$$\leq \int_a^b \|f\| \|K_{\mathbb{H}}(\cdot, x(t))v(t)\| dt \quad (63)$$

$$= \|f\| \int_a^b \|K_{\mathbb{H}}(\cdot, x(t))v(t)\| dt \quad (64)$$

$$= \|f\| \int_a^b \sqrt{v^T(t) K_{\mathbb{H}}(x(t), x(t)) v(t)} dt \quad (65)$$

For MOCK with $v(t) = e_k$, this simplifies to the condition

$$\int_a^b \sqrt{K_{\mathbb{H}}(x(t), x(t))_{k,k}} \leq \infty$$

for all k and trajectories $x(t)$. Note this is precisely the condition presented in Rielly et al. (2023). Thus the linear functionals are continuous under the very easy to satisfy condition that the square root of the kernel is finitely integrable on the intervals. Which is true for instance if $x(t)$ is bounded and integrable on $[a, b]$ and $K_{\mathbb{H}}$ is continuous (observe that it is always nonnegative as it is a kernel). Observing that $\Psi_{i,j,k}(\cdot) = e_k^T$, we may use 7 to immediately arrive at the solution to the optimization problem. We note that our bilinear forms look like:

$$p_{i,j,k}(f, v) = \int_{t_j^i}^{t_{j+1}^i} f(x^i(t))^T v(t) dt \quad (66)$$

and our linear functionals are:

$$l_{i,j,k}(v) = \int_{t_j^i}^{t_{j+1}^i} \dot{x}^i(t)^T v(t) dt \quad (67)$$

Thus 7 tells us

$$f(x) = \sum_{i=1}^n \sum_{j=1}^{n_i-1} \sum_{k=1}^d \sum_{l=1}^1 \alpha_{i,j,k,l} \mathcal{L}_{i,j,k,l}^*(*) \quad (68)$$

Notice all our test function spaces are one dimensional so our inner most sum is not a sum at all. We may evaluate $\mathcal{L}_{i,j,k,l}^*(*)$ from theorem 7 as follows:

$$\mathcal{L}_{i,j,k,l}^*(*) = \sum_{m=1}^d p_{i,j,k} (K_{\mathbb{H}}(\cdot, *) e_m, \Psi_{i,j,k}(\cdot)^T e_l) e_m \quad (69)$$

Since the test function spaces are one dimensional, the vector e_l is just the one dimensional scalar 1 (e_l has the same dimensions as the test function spaces). So we simplify to get:

$$\mathcal{L}_{i,j,k,l}^*(*) = \sum_{m=1}^d p_{i,j,k} (K_{\mathbb{H}}(\cdot, *) e_m, e_k) e_m \quad (70)$$

$$= \sum_{m=1}^d \left(\int_{t_j^i}^{t_{j+1}^i} (K_{\mathbb{H}}(x^i(t), *) e_m)^T e_k dt \right) e_m \quad (71)$$

So

$$f(x) = \sum_{i=1}^n \sum_{j=1}^{n_i-1} \sum_{k=1}^d \alpha_{i,j,k} \left(\sum_{m=1}^d \left(\int_{t_j^i}^{t_{j+1}^i} (e_m^T K_{\mathbb{H}}(*, x^i(t)) e_k) dt \right) e_m \right) \quad (72)$$

$$= \sum_{i=1}^n \sum_{j=1}^{n_i-1} \sum_{k=1}^d \alpha_{i,j,k} \left(\sum_{m=1}^d \int_{t_j^i}^{t_{j+1}^i} (e_m e_m^T K_{\mathbb{H}}(*, x^i(t)) e_k) dt \right) \quad (73)$$

$$= \sum_{i=1}^n \sum_{j=1}^{n_i-1} \sum_{k=1}^d \alpha_{i,j,k} \left(\int_{t_j^i}^{t_{j+1}^i} \left(\left(\sum_{m=1}^d e_m e_m^T \right) K_{\mathbb{H}}(*, x^i(t)) e_k \right) dt \right) \quad (74)$$

$$= \sum_{i=1}^n \sum_{j=1}^{n_i-1} \sum_{k=1}^d \alpha_{i,j,k} \left(\int_{t_j^i}^{t_{j+1}^i} (K_{\mathbb{H}}(*, x^i(t)) e_k) dt \right) \quad (75)$$

$$= \sum_{i=1}^n \sum_{j=1}^{n_i-1} \left(\int_{t_j^i}^{t_{j+1}^i} (K_{\mathbb{H}}(*, x^i(t))) dt \right) \vec{\alpha}_{i,j} \quad (76)$$

$$(77)$$

With

$$\vec{\alpha}_{i,j} \in \mathbb{R}^d, [\vec{\alpha}_{i,j}]_k = \alpha_{i,j,k}$$

This is exactly the form of the solution derived in Rielly et al. (2023). Let's complete our consideration by verifying that the linear system we solve is the same as the linear system presented in Rielly et al. (2023). 7 tells us to calculate α we solve the linear system

$$(M + \lambda I)\alpha = Y \quad (78)$$

Recalling that we index our occupation kernels ($\mathcal{L}_{i,j,k,l}^*$) with 4 indices. To simplify matters lets combine all these indices into one index and instead write \mathcal{L}_z^* . Then

$$M_{z:z'} = \langle \mathcal{L}_z^*, \mathcal{L}_{z'}^* \rangle \quad (79)$$

and

$$Y_z = l_{i,j,k}(\Psi_{i,j,k}(\cdot)^T e_l) = \int_{t_j^i}^{t_{j+1}^i} \dot{x}^i(t)^T (e_k^T)^T e_l dt \quad (80)$$

Recalling that $e_l = 1 \in \mathbb{R}$ we simplify to:

$$Y_z = \int_{t_j^i}^{t_{j+1}^i} \dot{x}^i(t)^T e_k dt \in \mathbb{R} \quad (81)$$

Reindexing to match the paper Rielly et al. (2023) and integrating we get:

$$Y_{i,j} = x^i(t_{j+1}^i) - x^i(t_j^i) \in \mathbb{R}^d \quad (82)$$

And we have:

$$M_{z:z'} = \sum_{o=1}^d p_{i,j,k}(p_{i',j',k'}(K_{\mathbb{H}}(\cdot, *)e_o, \Psi_{i',j',k'}(\cdot)^T e_{l'})e_o, \Psi_{i,j,k}(\cdot)^T e_l) \quad (83)$$

Proceeding forth recalling e_l and $e_{l'}$ are just the constant 1 and $\Psi_{i,j,k}(\cdot) = e_k^T$. We simplify to:

$$\sum_{o=1}^d p_{i,j,k}(p_{i',j',k'}(K_{\mathbb{H}}(\cdot, *)e_o, e_{k'})e_o, e_k) \quad (84)$$

Evaluating the bilinear functionals gives:

$$\begin{aligned} & \sum_{o=1}^d p_{i,j,k} \left(\int_{t_{j'}^i}^{t_{j'+1}^i} \left(K_{\mathbb{H}}(x^{i'}(t), *)e_o \right)^T e_{k'} dt \right) \\ &= \sum_{o=1}^d \left(\int_{t_j^i}^{t_{j+1}^i} \left(\int_{t_{j'}^i}^{t_{j'+1}^i} \left(K_{\mathbb{H}}(x^{i'}(t), x^i(\tau))e_o \right)^T e_{k'} d\tau \right) e_o \right)^T e_k d\tau \quad (85) \end{aligned}$$

Lastly, we will simplify (using the skew symmetry property of vector valued kernel functions) to get:

$$= \sum_{o=1}^d \left(\int_{t_j^i}^{t_{j+1}^i} \left(\int_{t_{j'}^{i'}}^{t_{j'+1}^{i'}} e_o^T K_{\mathbb{H}}(x^i(\tau), x^{i'}(t)) e_{k'} dt \right) e_o \right)^T e_k d\tau \quad (86)$$

$$= \sum_{o=1}^d \left(\int_{t_j^i}^{t_{j+1}^i} \left(\int_{t_{j'}^{i'}}^{t_{j'+1}^{i'}} e_{k'}^T K_{\mathbb{H}}(x^{i'}(t), x^i(\tau)) e_o dt \right) e_o \right)^T e_k d\tau \quad (87)$$

$$= \sum_{o=1}^d \int_{t_j^i}^{t_{j+1}^i} \int_{t_{j'}^{i'}}^{t_{j'+1}^{i'}} e_{k'}^T K_{\mathbb{H}}(x^{i'}(t), x^i(\tau)) (e_o e_o^T) e_k dt d\tau \quad (88)$$

$$= \int_{t_j^i}^{t_{j+1}^i} \int_{t_{j'}^{i'}}^{t_{j'+1}^{i'}} e_{k'}^T K_{\mathbb{H}}(x^{i'}(t), x^i(\tau)) \left(\sum_{o=1}^d e_o e_o^T \right) e_k dt d\tau \quad (89)$$

$$= \int_{t_j^i}^{t_{j+1}^i} \int_{t_{j'}^{i'}}^{t_{j'+1}^{i'}} e_{k'}^T K_{\mathbb{H}}(x^{i'}(t), x^i(\tau)) e_k dt d\tau \quad (90)$$

Considering the matrix M as a block matrix with $d \times d$ blocks (for the k index). We get:

$$M_{i,j:i',j'} = \int_{t_j^i}^{t_{j+1}^i} \int_{t_{j'}^{i'}}^{t_{j'+1}^{i'}} K_{\mathbb{H}}(x^{i'}(t), x^i(\tau)) dt d\tau \quad (91)$$

These are precisely the blocks given in equation (14) of Rielly et al. (2023).

4.5 Liouville Operator occupation kernel generalization

The idea of Occupation kernels, originally proposed in Rosenfeld et al. (2019), has been a topic of emerging literature for its remarkable flexibility. In the work Rosenfeld et al. (2024), the authors generalize the idea of the occupation kernel method using an idea relating to Liouville Operators. In this paper, it is proposed to minimize:

$$\inf_{u \in U} \left\| \int_0^T \nabla_2(k(\cdot, \gamma(t)))^T f(\gamma(t)) dt - \int_0^T \nabla_2(k(\cdot, \gamma(t)))^T u(\gamma(t)) dt \right\|_{\mathbb{V}}^2 \quad (92)$$

Where we adopt notation from Rosenfeld et al. (2024) in which ∇_2 indicates the gradient with respect to the second entry, $k(\cdot, *)$ is a scalar valued kernel function for a Reproducing Kernel Hilbert Space \mathbb{V} and U is a finite dimensional space of functions (characterized by a collection of basis functions) (See equation (7.1) Rosenfeld et al. (2024)). We present the unpacked version of equation (7.1) for self containment in equation 92. Let us show

$$\begin{aligned} \inf_{u \in U} \left\| \int_0^T \nabla_2(k(\cdot, \gamma(t)))^T f(\gamma(t)) dt - \int_0^T \nabla_2(k(\cdot, \gamma(t)))^T u(\gamma(t)) dt \right\|_{\mathbb{V}}^2 &\Leftrightarrow \\ \inf_{u \in U} \left\{ \sup_{v \in \mathbb{V}, \|v\|=1} \left\{ \left(\int_0^T \nabla(v(\gamma(t)))^T f(\gamma(t)) dt - \int_0^T \nabla(v(\gamma(t)))^T u(\gamma(t)) dt \right)^2 \right\} \right\} &\quad (93) \end{aligned}$$

Let's begin with

$$\inf_{u \in U} \left\{ \sup_{v \in \mathbb{V}, \|v\|=1} \left\{ \left(\int_0^T \nabla(v(\gamma(t)))^T f(\gamma(t)) dt - \int_0^T \nabla(v(\gamma(t)))^T u(\gamma(t)) dt \right)^2 \right\} \right\}$$

and show it is equivalent to 262. Here we see a bilinear form

$$\int_0^T \nabla(v(\gamma(t)))^T u(\gamma(t)) dt \quad (94)$$

of v and u and a linear functional

$$\int_0^T \nabla(v(\gamma(t)))^T f(\gamma(t)) dt \quad (95)$$

of v . The first thing we note is the authors of Rosenfeld et al. (2024) include a critical theorem in which they prove for every Lipschitz continuous function $f(\gamma(t))$, the operator

$$\int_0^T \nabla(v(\gamma(t)))^T f(\gamma(t)) dt$$

is bounded. Thus the linear functional and bilinear form are both bounded with respect to v (as well as U as U derives from a finite dimensional space). Proceeding as in the first step of the proof of theorem 7, we see that we may replace the supremum with 262 as desired (details are provided in the supplementary material).

There is an important difference between the formulation we present and the one presented in Rosenfeld et al. (2024). In Rosenfeld et al. (2024) the authors use two implicit kernels (infinite dimensional kernels) for the test function space. If the authors decide to use explicit (finite dimensional) kernels for the test function space, they recover an example of our formulation (without an explicit regularization term). This means our theorem is not directly applicable to provide the linear system, however, the candidate space of functions is finite dimensional. Moreover, the one critical point for the authors theory is that the linear functional

$$A_f^* g = \int_0^T \nabla_2(g(\gamma(t)))^T f(\gamma(t)) dt \quad (96)$$

is a bounded linear functional of g in the RKHS of test functions for any Lipschitz continuous f . This implies that the bilinear form is bounded in both terms and the linear functional is bounded as well. In this work we decide to focus on the case where the space of test functions is finite dimensional which is arguably the more natural case from a finite elements perspective.

5 ROCK (Riesz Occupation Kernel method)

With this general optimization framework, it becomes clear how one might seek to generalize some of the learning techniques that have recently been published. Consider the problem of learning dynamical systems from snapshots of trajectories (as presented in Rielly et al. (2023)). We seek $f(x(t))$ that satisfies

$$\dot{x}^i(t) = f(x^i(t)) \quad (97)$$

Suppose we have n trajectories, $x^1(t), \dots, x^n(t) \in \mathbb{R}^d$, and for each $i \in 1, \dots, n$ there are n_i samples of the trajectories. As we saw in 4.4, the MOCK method is an example of our optimization framework applied to the loss

$$\inf_{f \in \mathbb{H}} \left\{ \sum_{i=1}^n \sup_{\{v \in \mathbb{V}_i \mid \|v\|=1\}} \left\{ \left(\int_{a^i}^{b^i} f(x^i(t)) v(t) dt - \int_{a^i}^{b^i} \dot{x}^i(t)^T v(t) dt \right)^2 \right\} + \lambda \|f\|_{\mathbb{H}}^2 \right\} \quad (98)$$

Where here we have chosen to reindex for simplicity. In the original MOCK paper, the authors chose to integrate over one time step using two samples for the estimation of the integral and the trapezoid rule. They also chose to use a one dimensional RKHS of test functions proportional to e_j . In principal, we can integrate over any interval we wish and use any finite dimensional space of vector valued test functions we wish to use. Indeed, if we take numerical techniques as inspiration, we typically wish to make our space of test functions as expressive as it can be to get better convergence results. In addition, we may decide to use test functions with small support to potentially provide sparse linear systems. Proceeding from (98) we can apply 7 to get

$$f(*) = \sum_{i=1}^n \sum_{k=1}^q \alpha_{i,k} \left(\sum_{l=1}^d \left\{ \int_{a^i}^{b^i} (K_{\mathbb{H}}(x^i(t), *) e_l)^T (\Psi_i^T(t) e_k) dt \right\} e_l \right) \quad (99)$$

$$= \sum_{i=1}^n \sum_{k=1}^q \alpha_{i,k} \left(\sum_{l=1}^d \left\{ \int_{a^i}^{b^i} e_l^T K_{\mathbb{H}}(*, x^i(t)) (\Psi_i^T(t) e_k) dt \right\} e_l \right) \quad (100)$$

$$= \sum_{i=1}^n \sum_{k=1}^q \alpha_{i,k} \left(\sum_{l=1}^d e_l \left\{ e_l^T \int_{a^i}^{b^i} K_{\mathbb{H}}(*, x^i(t)) (\Psi_i^T(t) e_k) dt \right\} \right) \quad (101)$$

$$= \sum_{i=1}^n \sum_{k=1}^q \alpha_{i,k} \left(\sum_{l=1}^d (e_l e_l^T) \right) \left\{ \int_{a^i}^{b^i} K_{\mathbb{H}}(*, x^i(t)) (\Psi_i^T(t) e_k) dt \right\} \quad (102)$$

$$= \sum_{i=1}^n \sum_{k=1}^q \alpha_{i,k} \left\{ \int_{a^i}^{b^i} K_{\mathbb{H}}(*, x^i(t)) (\Psi_i^T(t)) dt \right\} e_k \quad (103)$$

$$= \sum_{i=1}^n \left\{ \int_{a^i}^{b^i} K_{\mathbb{H}}(*, x^i(t)) (\Psi_i^T(t)) dt \right\} \vec{\alpha}_i \quad (104)$$

$$(105)$$

Where we are able to move the e_l vector to the front in 101 because the term in the curly braces is a scalar valued function. Here, for every trajectory indexed by i , we may choose to evaluate p_i integrals with different test function spaces for each integral, and the test function spaces are spaces of functions from t to \mathbb{R}^d , thus providing the term involving the sum over l . q denotes the dimensionality of the test function space. For simplicity we choose q to be the same for all our test function spaces but nothing stops an engineer from choosing

different dimensionalities for each test function space as well. 7 also tells us that we may obtain $\alpha_{i,j,k}$ by solving the linear system

$$(M + \lambda I) \alpha = Y \quad (106)$$

with

$$Y_{i,k} = \int_{a^i}^{b^i} \dot{x}^i(t)^T \Psi_i(t)^T e_k dt \quad (107)$$

so that

$$\vec{Y}_i = \int_{a^i}^{b^i} \Psi_i(t) \dot{x}^i(t) dt \quad (108)$$

and

$$M_{i,k:i',k'} \quad (109)$$

$$= \sum_{l=1}^d \int_{a^i}^{b^i} \left\{ \left[\int_{a^{i'}}^{b^{i'}} \left((K_{\mathbb{H}}(x^{i'}(\tau), x^i(t)) e_l)^T \Psi_{i'}(\tau)^T e_{k'} \right) d\tau \right] e_l \right\}^T \Psi_i(t)^T e_k dt \quad (110)$$

$$= \sum_{l=1}^d \int_{a^i}^{b^i} \left\{ \left[\int_{a^{i'}}^{b^{i'}} \left(e_l^T K_{\mathbb{H}}(x^i(t), x^{i'}(\tau)) \Psi_{i'}(\tau)^T e_{k'} \right) d\tau \right] e_l \right\}^T \Psi_i(t)^T e_k dt \quad (111)$$

$$= \sum_{l=1}^d \int_{a^i}^{b^i} \left[\int_{a^{i'}}^{b^{i'}} \left(e_{k'}^T \Psi_{i'}(\tau) K_{\mathbb{H}}(x^{i'}(\tau), x^i(t)) e_l \right) d\tau \right] e_l^T \Psi_i(t)^T e_k dt \quad (112)$$

$$= \sum_{l=1}^d \int_{a^i}^{b^i} \int_{a^{i'}}^{b^{i'}} \left(e_{k'}^T \Psi_{i'}(\tau) K_{\mathbb{H}}(x^{i'}(\tau), x^i(t)) \right) d\tau \left(e_l e_l^T \right) \Psi_i(t)^T e_k dt \quad (113)$$

$$= \int_{a^i}^{b^i} \int_{a^{i'}}^{b^{i'}} \left(e_{k'}^T \Psi_{i'}(\tau) K_{\mathbb{H}}(x^{i'}(\tau), x^i(t)) \right) d\tau \left(\sum_{l=1}^d e_l e_l^T \right) \Psi_i(t)^T e_k dt \quad (114)$$

$$= \int_{a^i}^{b^i} \int_{a^{i'}}^{b^{i'}} e_{k'}^T \Psi_{i'}(\tau) K_{\mathbb{H}}(x^{i'}(\tau), x^i(t)) \Psi_i(t)^T e_k d\tau dt \quad (115)$$

Keep in mind the term in the brackets is scalar valued so we can take its transpose without changing the value. So that the $M_{i:i'}$ th block is

$$\int_{a^i}^{b^i} \int_{a^{i'}}^{b^{i'}} \Psi_{i'}(\tau) K_{\mathbb{H}}(x^{i'}(\tau), x^i(t)) \Psi_i(t)^T d\tau dt \quad (116)$$

In our implementation we choose

$$K_{\mathbb{H}}(\cdot, *) = k(\cdot, *) I_d \quad (117)$$

and

$$\Psi_i(t) = \vec{\psi}_i(t) \otimes I_d \in \mathbb{R}^{pd \times d} \quad (118)$$

Where \otimes denotes the Kronecker product. This choice of Ψ is equivalent to using

$$K(\cdot, *) = \Psi_i(\cdot)^T \Psi_i(*) \quad (119)$$

$$= (\psi_i(\cdot) \otimes I_d)^T (\psi_i(*) \otimes I_d) \quad (120)$$

$$= (\psi_i(\cdot)^T \psi_i(*)) \otimes (I_d^T I_d) \quad (121)$$

$$= \psi_i^T(\cdot) \psi_i(*) I_d \quad (122)$$

A seperable kernel proportional to the identity using the finite dimensional explicit kernel $\psi_i(\cdot)^T \psi_i(*)$. So for a scalar kernel with p features, the vvRKHS of test functions we use is pd dimensional.

5.1 Vectorizations and Optimizations

Before we can arrive at the final implementation details, we require some further simplification. We dedicate an entire subsection to this because this is the heart of what allows the ROCK algorithm to be so remarkably concise and practically efficient to run. We expect similar optimizations may be applied to many other losses derived from our framework.

Recall for ROCK we need to solve the linear system

$$(M + \lambda I)\alpha = Y \quad (123)$$

where

$$Y \in \mathbb{R}^{npd} \quad (124)$$

with

$$Y_i = \int_{a^i}^{b^i} \Psi_i(t) \dot{x}^i(t) dt = \int_{a^i}^{b^i} (\psi_i(t) \otimes I) \dot{x}^i(t) dt \quad (125)$$

On the other hand, the i, i' th block of the matrix M is given by

$$\int_{a^i}^{b^i} \int_{a^{i'}}^{b^{i'}} \Psi_{i'}(\tau) K_{\mathbb{H}}(x^{i'}(\tau), x^i(t)) \Psi_i(t)^T d\tau dt \quad (126)$$

$$= \int_{a^i}^{b^i} \int_{a^{i'}}^{b^{i'}} (\psi_{i'}(\tau) \otimes I) \left(k(x^{i'}(\tau), x^i(t)) I \right) (\psi_i(t) \otimes I)^T d\tau \quad (127)$$

$$= \int_{a^i}^{b^i} \int_{a^{i'}}^{b^{i'}} k(x^{i'}(\tau), x^i(t)) (\psi_{i'}(\tau) \otimes I) (\psi_i(t) \otimes I)^T dt d\tau \quad (128)$$

$$= \int_{a^i}^{b^i} \int_{a^{i'}}^{b^{i'}} k(x^{i'}(\tau), x^i(t)) (\psi_{i'}(\tau) \psi_i(t)^T \otimes I) dt d\tau \quad (129)$$

$$= \left(\int_{a^i}^{b^i} \int_{a^{i'}}^{b^{i'}} \left(k(x^{i'}(\tau), x^i(t)) \psi_{i'}(\tau) \psi_i(t)^T \right) dt d\tau \right) \otimes I \quad (130)$$

$$\approx \left(\sum_{k=1}^n \sum_{j=1}^m q_k q_j \left(k(x^{i'}(\tau_k), x^i(t_j)) \psi_{i'}(\tau_k) \psi_i(t_j)^T \right) \right) \otimes I \quad (131)$$

where q_k and q_j are weights derived from the choice of numerical quadrature. If we let $K^{i',i}$ be the gram matrix $K_{j:k}^{i',i} = k(x^{i'}(\tau_k), x^i(t_j))$, and $q\Psi_t$ and $q\Psi_\tau$ be matrices associated with the feature functions and quadratures $[q\Psi_\tau]_k = q_k\psi_{i'}(\tau_k) \in \mathbb{R}^q$ then we can estimate all the terms of the integral by evaluating the matrix multiplications

$$(q\Psi_\tau)K^{i',i}(q\Psi_t)^T \quad (132)$$

In addition, a linear system of the form

$$(M \otimes I)\alpha = Y \quad (133)$$

such as our linear system, may be rewritten using properties of Kronecker products as

$$M\alpha' = Y' \quad (134)$$

where α' and Y' are matrix valued and α and Y are flattened versions of α' and Y' . This allows us to solve a much smaller linear system.

6 Methods And Experiments

We generalized MOCK (referred to as ROCK) and benchmark against MOCK from Rielly et al. (2023) (we refer to as MOCK) comparing on the same datasets with the same training procedures. Our scores are benchmarked against the models presented in Rielly et al. (2023).

6.1 Datasets

We test the methods on a diverse collection of synthetic datasets following the benchmarks in Rielly et al. (2023). These datasets include data up to 1024 dimensions, as well as synthetic data with noise, and without noise.

Noisy Fitz-Hugh Nagumo (NFHN) The FitzHugh-Nagumo oscillator FitzHugh (1961) is a nonlinear 2D dynamical system that models the basic behavior of excitable cells, such as neurons and cardiac cells Rielly et al. (2023). This dataset arises from a well specified dynamical system of the form we model, but contains considerable levels of noise (see the supplementary materials for a figure).

Noisy Lorenz63 (Lorenz63) The Lorenz63 system Lorenz (1963) is a 3D system provided as a simplified model of atmospheric convection. This dataset, constructed for the benchmarks in Rielly et al. (2023), also contains added noise.

Lorenz96 The Lorenz96 data arises from Lorenz (1995) in which a system of equations is proposed that may be chosen to have any dimension greater than 3. (Lorenz96-16) has 16 dimensions, etc.

The synthetic data we benchmark against includes Lorenz96 of dimension 16, 32, 128 and 1024 (containing no noise), Lorenz63 and FHN (containing added noise). Each of these synthetic datasets arise from a true model that matches the model assumptions of MOCK so we expect MOCK to perform well on these datasets which is indeed what we find.

Table 2: Datasets

Name	Type	d	n	m
NFHN	Synthetic	2	150	201
Lorenz63	Synthetic	3	150	201
Lorenz96-16	Synthetic	16	100	81
Lorenz96-32	Synthetic	32	100	81
Lorenz96-128	Synthetic	128	100	81
Lorenz96-1024	Synthetic	1024	100	100

Table 3: d denotes the dimension of the dynamical system, n the number of trajectories and m the average number of samples per trajectory. This table was taken from Rielly et al. (2023)

6.2 Validation

For each of the datasets, we use a Gaussian, Laplace, and Matern kernel as our scalar kernel. These are all implicit radial basis kernels with the forms

$$g(r) = e^{-\frac{r^2}{2\sigma^2}} \quad (135)$$

$$l(r) = e^{-\frac{r}{\gamma}} \quad (136)$$

and

$$m(r) = \frac{e^{-\frac{r}{\gamma}}}{945} \left(\left(\frac{r}{\gamma}\right)^5 + 15 \left(\frac{r}{\gamma}\right)^4 + 105 \left(\frac{r}{\gamma}\right)^3 + 420 \left(\frac{r}{\gamma}\right)^2 + 945 \frac{r}{\gamma} + 945 \right) \quad (137)$$

where $r = \|x - y\|$ and γ and σ are referred to as the scale parameters.

We use legendre polynomials for our feature functions as our scalar kernel for the test function space. For each trajectory, the legendre polynomials are scaled and shifted to fit the time frame of the trajectory. This implies our RKHS of test functions is a subspace of $L^2(a, b)$ for any trajectory going from time a to time b .

For each of the 3 kernels, and for test function spaces with 1 to 7 features, we trained and validated on the training and validation sets (60% training 20% validation 20% test). We learn the regularization parameter and scale parameter that has the best performance on the validation set. We then selected the choice of kernel and number of features that had the best performance on the validation set. We report the performance of this model on the test set. For the Lorenz96 16, 32, and 128 datasets, we additionally cut the trajectories in approximately 7 cuts and 10 cuts for Lorenz96 1024. We do validation on this training set as well. Cutting trajectories into smaller pieces results in effectively an additional hyper parameter that can be tuned. Cutting trajectories into 2 sample trajectories for instance recovers the original MOCK algorithm.

Thus, the riesz OCK (*ROCK*) results reported in 4 are the results of the best performing ROCK model on the validation set when we consider the three choices of kernels, the choice of 1, 2, ..., 7 dimensional test function spaces, and for lorenz96 datasets, the choice of longer or shorter trajectories in the training set.

Table 4: Dynamical System Estimation Results

Lorenz63			NFHN			Lorenz96-16		
	Err	1-Err		Err	1-Err		Err	1-Err
ResNet	2.07	.014	ResNet	5.94	.064	ResNet	6.42	.010
eDMD-Deep	2.9	.009	eDMD-Deep	4.54	.036	eDMD-Deep	5.93	.040
eDMD-Poly	2.22	.012	eDMD-Poly	4.10	.037	eDMD-Poly	6.91	.036
eDMD-RFF	1.93	.011	eDMD-RFF	4.01	.037	eDMD-RFF	6.22	.029
null	2.56	.011	null	9.69	.043	null	7.50	.039
SINDy-Poly	.99	.002	SINDy-Poly	1.68	.022	SINDy-Poly	.40	.0003
mockG	.66	.002	mockG	1.40	.029	mockG	.69	.0007
mockL	.65	.002	mockL	1.11	.030	mockL	.22	.0001
mockM	2.52	.012	mockM	1.41	.029	mockM	.22	.0001
mockF	2.52	.012	mockF	1.38	.028	mockF	.22	.0001
ROCK	.51	.001	ROCK	.41	.012	ROCK	.13	.0001
Lode	1.49	.092	Lode	.64	.131	Lode	3.82	.138
Lorenz96-32			Lorenz96-128			Lorenz96 -1024		
	Err	1-Err		Err	1-Err		Err	1-Err
ResNet	11.56	.020	ResNet	24	2.64	ResNet	66.1	6.48
eDMD-Deep	8.79	.057	eDMD-Deep	17	.089	eDMD-Deep	26.9	.41
eDMD-Poly	9.67	.051	eDMD-Poly	19	.109	eDMD-Poly	61.5	.42
eDMD-RFF	8.10	.028	eDMD-RFF	16	.201	eDMD-RFF	54.2	.38
null	10.49	.056	null	21	.112	null	67.0	.16
SINDy-Poly	8.56	.037	SINDy-Poly	19	.066	SINDy-Poly	NA	NA
mockG	.47	.0001	mockG	17	.064	mockG	18.0	.013
mockL	.48	.0001	mockL	16	.035	mockL	17.8	.014
mockM	.49	.0001	mockM	16	.040	mockM	17.9	.013
mockF	.47	.0001	mockF	16	.036	mockF	18.0	.015
ROCK	.41	.0001	ROCK	15	.019	ROCK	17.0	.014
Lode	6.06	.217	Lode	15	.342	Lode	15.8	1.04

Description: Minimum values are in bold. Our models are labeled as mockG - original occupation kernel method with Gaussian kernel, mockM - original occupation kernel method with Matern kernel, mockF - original occupation kernel method with Random Fourier Features (RFF), mockL - original occupation kernel with Laplace kernel and ROCK - our generalized weak occupation kernel method (Gaussian, Laplace, and Matern kernels as well as number of test features selected as the best performing options on the validation set). We compare against SINDy-Poly, eDMD-Deep, eDMD-Poly, eDMD-RFF, ResNet and Latent Ode (Lode) (See 6.1). No result could be obtained for SINDy-Poly for Lorenz96 1024.

6.3 Legendre Polynomial test Functions

For our explicit (finite dimensional) space of test functions we use the legendre polynomials as basis functions and the L^2 inner product to define our vvRKHS. The Legendre polynomials are given by taking the basis polynomials:

$$1, x, x^2, \dots \quad (138)$$

and making them orthogonal with respect to the $L^2([-1, 1])$ inner product. We scale and shift these polynomials for each intervals of integration to provide polynomials that are

orthonormal with respect to $L^2(a, b)$. Thus our RKHS of test functions is a finite dimensional subspace of $L^2(a, b)$

6.4 Runtime

For all runtime calculations, refer to the python code presented for ROCK in the supplementary section. In training time, we find empirically, the computational bottlenecks to be the construction of the gram matrix G , the multiplication of G with the block diagonal matrices Φ^T and Φ , and solving the linear system: $(M + \lambda I)\alpha = Y$ where $a, Y \in \mathbb{R}^{n \times d}$. Letting n be the number of trajectories, p be the number of features of the test function space, m be the number of points in each trajectory, and d be the dimensionality of the dynamical system, we get the following runtimes for each of these three operations: To compute G , we require a $nm \times d$ by $d \times nm$ matrix matrix multiplication (as we use a radial basis implicit kernel). Thus, construction of G is upper bounded asymptotically by $O((nm)^2 d)$ where $nm = N$ is the total number of datapoints in the training set. Since $\Phi \in \mathbb{R}^{np \times nm}$ is block diagonal $G \cdot \Phi^T$ can be computed by n matrix matrix multiplications of the shape $nm \times p$ by $p \times m$. These can be done in parallel to save time at the expense of the requirement of additional space. Therefore, the calculation of $\Phi \cdot (G \cdot \Phi^T)$ requires $O((nm)^2 p)$. Finally, we solve d linear systems (which may also be solved simultaneously). Each linear system is of dimension np . In principle, a linear system of dimension $n \times n$ may be solved with the same computational complexity as an $n \times n$ by $n \times n$ matrix matrix multiplication (about $O(n^{2.5})$ in practice though lower in principle). However in practice, algorithms for solving linear systems have somewhat worse runtimes. Let's make a conservative estimate of $O(n^3)$. Thus, the runtime to solve the linear system is $O((np)^3 d)$. We get the total runtime for training of:

$$O((np)^3 d + (nm)^2 p + (nm)^2 d) \quad (139)$$

In our experiments, the number of test function features is always kept fairly low (less than 10), so we can ignore p in our analysis and we get the runtime:

$$O((n^3 + (nm)^2) d) \quad (140)$$

We see, so long as the number of samples per trajectory is less than or equal to \sqrt{n} (the square root of the number of trajectories), the first term dominates the asymptotics, otherwise the second term dominates.

6.5 Important Note on Runtime

This generalization of the MOCK algorithm allows the user to reduce the length of the trajectories used in integration by cutting long trajectories into smaller trajectories. If long trajectories are used, our models become fairly sparse (containing few parameters) compared with other models such as MOCK. This can greatly reduce the runtime of our generalized algorithm. For example, while the MOCK model trained on the lorenz63 dataset has approximately 20000×3 parameters and requires solving 20000×20000 linear systems, our generalized ROCK algorithm not only outperformed this model, but it did so using only 100×3 parameters. MOCK requires about d parameters per sample while our ROCK

model only requires d parameters per trajectory. For problems involving datasets of long trajectories, this allows the user the ability to test different model sizes for performance by cutting the long trajectories into different lengths of shorter trajectories.

6.6 Runtime For Inference

For inference, if we wish to evaluate f at l new samples, we first have to create a gram matrix of shape $l \times nm$. This requires (among other less intensive computations) a matrix multiplication of an $l \times d$ and a $d \times nm$ matrix. We can bound the runtime of this multiplication to $O(lnmd)$. Next, we must multiply G by $QPhi$. Which has a runtime of $O(nlmp)$. This results in the matrix $G \cdot QPhi.T$ of shape $l \times np$. We multiply the transpose of this matrix by the transpose of $\alpha \in \mathbb{R}^{np \times d}$, to get an additional $O(dnpl)$ term. Thus, for one evaluation of f at l samples, we require

$$O(nl(md + mp + pd)) \quad (141)$$

Assuming again that p is negligible, we see that the bottleneck of the evaluation is the computation of the gram matrix, and we get an inference runtime of

$$O(nlmd) \quad (142)$$

Integration of the slopefield for t steps to obtain trajectories, will give us the inference runtime of:

$$O(nlmdt) \quad (143)$$

7 Ablation Study

In addition to the experiments in 6 we benchmark ROCK on the datasets provided by the Common Task Framework (CTF) of the AI Institute for Dynamical Systems [1].

We focus on the task 1 challenge (forecasting the dynamical system over a short time frame) for datasets derived from 4 different dynamical systems.

Double Pendulum This dataset provides angle and angular momentum measurements of the dynamics derived from a double pendulum. The data we are provided contains one trajectory with 2000 samples.

Lorenz63 This dataset provides evenly sampled samples from the lorenz63 dynamical system. We are provided 2000 samples from one trajectory.

Rosler this is also a three dimensional dynamical system designed to have similar chaotic behavior as the lorenz attractor but be easier to analyze.

Kolmogorov Arises from a two dimensional partial differential equation. Each measurement across the x axis is taken to be a new dimension and each measurement in time is taken to be the time axis of the dynamical system. In this way solutions to PDEs may be characterized as dynamical systems. However, as the number of measurements in the x axis increase the dimensionality of the system grows very quickly. In this example, the dynamical system is more than 16000 dimensional.

7.1 Method

Each dataset provides us with one trajectory that has 2000 samples. In our validation procedure for learning the dynamics we consider test function spaces ranging from 1 to 7 dimensions. We split the training set into a 1200 train, 400 validate and 400 test set. We use the 1200 training and 400 validation points to select our model, and our hyperparameters. Then we retrain with this model and these hyperparameters taking the 1200 train and 400 validate samples as our new training set and the 400 test samples as our validation set. The model learned from this final step is published to the competition.

The hyperparameters we have for our model are:

1. The number of test features
2. The number of training trajectories to cut the training set into
3. The number of validation trajectories to cut the validation set into.
4. The choice of kernel
5. The scale parameter for the kernel.
6. the regularization term for the model.

The choice of test function space and trajectory length determines the number of parameters of the learned model. The number of parameters increases linearly with the number of trajectories, the number of test features and the number of dimensions. This is demonstrated in 5.

7.2 Competition tentative results:

We published our model results on the platform for the first task in the competition [1]. This task requires us to use the provided 2000 samples of one trajectory of each dynamical system to learn the dynamical system and forecast the next 2000 samples. Our forecasts are evaluated on their ability to do short term prediction of the dynamical system using the error:

$$E1 = \left(1 - \frac{\sum_{i=1}^n \|\hat{x}(t_i) - x(t_i)\|^2}{\sum_{i=1}^n \|x(t_i)\|^2} \right) \cdot 100 \quad (144)$$

Here, $\hat{x}(t_i)$ is the predicted trajectory evaluated at t_i , and $x(t_i)$ is the true trajectory evaluated at t_i . This error is a linear transformation of the error we report for our experiments in 4, but has the nice properties that a model that has the same performance as null model ($x(t) = 0$) will evaluate to 0, a model that has perfect performance will evaluate to 100 and a model that has worse than trivial performance will evaluate to less than 0. Thus, these experiments did not require publishing results for the null model. In addition, the platform evaluates the long term performance of the predicted model by taking the fourier transform of the trajectories, truncating all but the lowest 100 frequencies and reporting the RMSE between the lower part of the power spectrum of the predicted and true models (see [1]).

$$E2 = \left(1 - \frac{\sum_{i=1}^{100} \left\| \ln \left(|FFT(\hat{x})(z_i)|^2 \right) - \ln \left(|FFT(x)(z_i)|^2 \right) \right\|^2}{\sum_{i=1}^{100} \left\| \ln \left(|FFT(x)(z_i)|^2 \right) \right\|^2} \right) \cdot 100 \quad (145)$$

Where $FFT(x(t_1))$ is the fourier transform of the constant function and $FFT(x)(z_i)$ is the z_i th frequency of the fourier transform of $x(t)$. MOCK and ROCK models currently outperform all other submissions to the competitions on both metrics for the first task, however the deadline for the competition does not pass until 2026 so we expect many more entries to arrive. In table 10 we compare the errors of our best performing ROCK submission to the best performing MOCK submission. We see while the E1 errors tend to be similar for both types of models, the E2 errors can sometimes be much better with the ROCK models. It is worth noting that all datasets here are noise free, but ROCK models tend to have far fewer parameters which likely results in better generalization to long time frames as is evidenced by the better E2 errors.

	<i>Length</i>	2	5	10	15	25	50	75	300	600
<i>features</i>	1	9.8M	3.9M	2.0M	1.3M	.79M	.39M	.26M	66T	33T
	2	20M	7.8M	4.0M	2.6M	1.6M	.78M	.52M	.13M	66T
	3	29M	12M	6.0M	3.9M	2.4M	1.2M	.78M	.20M	99T
	4	39M	16M	8.0M	5.2M	3.2M	1.6M	1.04M	.26M	.13M
	5	49M	20M	10M	6.5M	4.0M	2.0M	1.3M	.33M	.17M
	6	59M	23M	12M	7.8M	4.7M	2.3M	1.6M	.40M	.20M
	7	69M	27M	14M	9.1M	5.5M	2.7M	1.8M	.46M	.23M

Table 5: The number of parameters (K denotes thousands M millions) in the ROCK model for each choice of trajectory length in the training set and test feature number for the Kolmogorov dataset. The number of trajectories in the training set is given as the ratio of 1200 and the length of the trajectories. Notice all other datasets will have similar parameter counts (after scaling by the number of dimensions)

	<i>Train length</i>	2	5	10	15	25	50	75	300	600
<i>features</i>	1	56	57	57	58	61	56	58	72	73
	2	58	57	57	57	58	59	54	71	72
	3	71	65	67	68	56	58	60	70	72
	4	71	71	58	59	63	55	59	59	70
	5	71	71	55	64	67	55	57	48	69
	6	71	71	71	71	55	53	54	49	70
	7	71	71	67	58	58	54	60	58	69

Table 6: The validation performance (E1 144) of the ROCK model for each choice of trajectory length in the training set and test feature number for the Kolmogorov dataset. On the top left is the validation performance for ROCK with hyperparameters consistent with the original MOCK implementation (1 feature and 2 sample training trajectories). We see for most choices of features and trajectory lengths we can outperform on the validation set with ROCK.

	<i>Train length</i>	2	5	10	15	25	50	75	300	600
<i>features</i>	1	90	84	83	92	92	86	93	77	90
	2	84	86	84	84	82	87	92	79	71
	3	90	85	84	85	83	86	87	93	82
	4	74	81	83	85	83	83	87	84	79
	5	90	90	85	89	83	85	86	71	85
	6	4	84	82	85	84	84	84	90	90
	7	90	90	89	88	90	84	84	85	90

Table 7: The validation performance (E1 144) of the ROCK model for each choice of trajectory length in the training set and test feature number for the double pendulum dataset. On the top left is the validation performance for ROCK with hyper-parameters consistent with the original MOCK implementation (1 feature and 2 sample training trajectories). Here the original MOCK will perform competitively. ROCK will often provide very small but performant models. In this case, one of the best performing models (300 sample training trajectories, with 3 test features) learns a model for the double pendulum with $\frac{1200}{300} \cdot 3 \cdot 2 = 24$ parameters, while the model for 600 sample training trajectories, with 1 test function has just 8 parameters but performs equal to or better than all but 5 of the models, by contrast, the original MOCK model for this dataset has 2400 parameters.

	<i>Train length</i>	2	5	10	15	25	50	75	300	600
<i>features</i>	1	39	37	37	33	32	39	30	41	7
	2	34	36	36	36	34	35	33	34	30
	3	18	42	40	36	41	32	30	36	29
	4	35	41	36	50	34	35	37	35	34
	5	23	40	39	33	38	41	35	32	31
	6	35	30	36	37	46	38	41	31	35
	7	8	16	28	37	37	41	34	30	30

Table 8: The validation performance (E1 144) of the ROCK model for each choice of trajectory length in the training set and test feature number for the lorenz dataset. On the top left is the validation performance for ROCK with hyper-parameters consistent with the original MOCK implementation (1 feature and 2 sample training trajectories). Although the original MOCK score is good (39%) there is another choice of parameters that performs much better (50%).

8 Concluding Remarks

We provide a representer theorem for losses derived from weak formulations and demonstrate how many standard numerical and machine learning losses can be thought of as applications of these weak formulations. In this general framework it becomes more clear how one may construct new losses for new learning and numerical problems as well as how one may generalize existing losses. We provide an example in which we generalize a loss from the

	<i>Train length</i>	2	5	10	15	25	50	75	300	600
<i>features</i>	1	98	98	98	98	99	96	93	−5	−75
	2	92	97	97	97	99	98	99	4	−43
	3	−2	2	88	87	98	93	98	82	34
	4	16	−54	61	85	98	89	99	96	23
	5	−2	−2	−4	84	97	85	99	94	88
	6	9	4	−52	26	82	89	100	95	94
	7	1	−5	0	−41	67	84	99	91	80

Table 9: The validation performance (E1 144) of the ROCK model for each choice of trajectory length in the training set and test feature number for the Rosseler dataset. On the top left is the validation performance for ROCK with hyper-parameters consistent with the original MOCK implementation (1 feature and 2 sample training trajectories).

<i>E1</i>	<i>DP</i>	<i>KMG</i>	<i>LR</i>	<i>RS</i>	<i>E2</i>	<i>DP</i>	<i>KMG</i>	<i>LR</i>	<i>RS</i>
<i>MOCK</i>	97.27	90.71	97.24	99.98	<i>MOCK</i>	83.70	88.18	60.2	87.40
<i>ROCK</i>	96.63	90.11	99.1	99.98	<i>ROCK</i>	94.78	94.81	83.95	85.97

Table 10: When we compare the MOCK performance to the ROCK performance on the datasets from the synapse competition we see ROCK outperforms MOCK in 5 of the 8 cases. Moreover, we see this performance difference is more evident in the E2 scores where the performance gap is as much as 23% while the biggest advantage we ever see from MOCK does not appear to be significant (less than 2%). This is in agreement with the observation that the models learned with ROCK have much fewer parameters and should generalize better over longer time frames. In addition, ROCK is a true generalization of MOCK and thus proper and complete hyper-parameter tuning of ROCK should always ensure ROCK at least matches MOCK.

MOCK method and demonstrate that the learned models are both smaller (in terms of the number of parameters) and often better. We expect consistency and convergence theory to flow more naturally in this general framework.

8.1 Model Performance and Sparsity

We observe remarkable improvement of our generalized model on the noisy synthetic datasets. Where prior best performance on Lorenz63 was also by an occupation kernel model, we beat prior best performance reducing the error on the test set from .65 to .51. Our performance improvement for the Noisy FHN dataset was even more pronounced, reducing the error from 1.11 down to .41 (now the best performing model in our benchmark). A great improvement of performance was also observed for the Lorenz96-16 dataset. In addition, while the MOCK

method has a parameter count that scales linearly with the product of d and the number of samples, the more general ROCK method has a parameter count that scales linearly with the product of d and the number of trajectories. Referring to table 2 we may conclude that these, more performant models, have a parameter count that is 81 to 201 times smaller than the original MOCK models. We believe the additional sparsity of solution provided by these ROCK models may be one of the reasons why we are able to perform so well on the noisy synthetic datasets.

Table 9 is instructive to look at. For very short training trajectories, it does one no good to look at high dimensional feature spaces. This is like trying to integrate high order polynomials with only 2 samples. This results in an overdetermined system with too many parameters and too few degrees of freedom. In this case we can see poor behavior or unstable results (regularization helps). For very long trajectories and low dimensional feature spaces, the total number of parameters starts becoming very small and the model may not be expressive enough to learn the dynamics. While the sweet spot may be found somewhere in the middle with somewhat long trajectories and a handful of test feature functions.

8.2 Future Work

This framework opens the doors for many followup questions some of which we share here. Our formulation optimizes over finite dimensional test function spaces and arbitrary RKHSs of candidate functions, what does the case of arbitrary RKHSs of test functions look like (as in the case of Rosenfeld et al. (2024))? How does the quadrature we chose for integration impact our integral accuracies? Can we provide numerical consistency results? In other words, how accurately can we estimate the solution in the case of noise free data? Can we provide convergence results? In other words how many samples are required to get adequate estimates of the solution in the case of noisy data? For these standard questions how much needs to be assumed of the RKHSs, linear functionals and bilinear functionals in order for the consistency and convergence results to be proven? Can they be proven in a general context such as the representer theorem or do they require case by case arguments? What does the application of RKHSs to numerical problems allow us to do with finite elements and Galerkin methods? Does it simplify the proofs? Does it provide any new insights? Lastly, perhaps the most exciting question, what other problems can we tackle with this approach? Can we learn PDE's, solve PDE's, learn dynamics arising from more interesting systems of differential equations? What nonlinear extensions are there?

Appendix A. Existence and uniqueness

Proposition 5 *Let \mathbb{H} be a Hilbert space of vector valued functions where for each $f, g \in \mathbb{H}$, $f(x) \in \mathbb{R}^d$ takes $x \in \mathcal{X}$ to \mathbb{R}^d with real valued inner product $\langle f, g \rangle_{\mathbb{H}} \in \mathbb{R}$. And let $\{b_1(x), \dots, b_n(x)\}$ be an orthonormal basis for this Hilbert space of functions. Then \mathbb{H} is a vector valued RKHS with kernel function*

$$K_{\mathbb{H}}(x, y) = \Psi(x)^T \Psi(y) \quad (146)$$

where

$$\Psi(x) = \begin{bmatrix} b_1(x)^T \\ \vdots \\ b_n(x)^T \end{bmatrix} \quad (147)$$

Proof That \mathbb{H} shares the same set of functions as the RKHS is obvious, indeed $f \in \mathbb{H}$ iff $f(x) = \sum_{i=1}^n \alpha_i b_i(x) = \Psi(x)^T \alpha$. All that remains to prove is the reproducing property. Let $f(\cdot) = \sum_{i=1}^n \alpha_i b_i(\cdot) = \Psi(\cdot)^T \alpha \in \mathbb{H}$ and $v \in \mathbb{R}^d$ be arbitrary, we must show

$$v^T f(x) = \langle f, \Psi(\cdot)^T \Psi(x) v \rangle_{\mathbb{H}} \quad (148)$$

$$\langle f, \Psi(\cdot)^T \Psi(x) v \rangle = \left\langle \sum_{i=1}^n \alpha_i b_i(\cdot), [b_1(\cdot), \dots, b_n(\cdot)] \begin{bmatrix} b_1(x)^T v \\ \vdots \\ b_n(x)^T v \end{bmatrix} \right\rangle \quad (149)$$

$$= \left\langle \sum_{i=1}^n \alpha_i b_i(\cdot), \sum_{i=1}^n (b_i(x)^T v) b_i(\cdot) \right\rangle \quad (150)$$

$$= \sum_{i=1}^n \sum_{j=1}^n \langle \alpha_i b_i(\cdot), (b_j(x)^T v) b_j(\cdot) \rangle \quad (151)$$

$$= \sum_{i=1}^n \alpha_i (b_i(x)^T v) \langle b_i(\cdot), b_i(\cdot) \rangle \quad (152)$$

$$= \sum_{i=1}^n \alpha_i (b_i(x)^T v) \quad (153)$$

$$= v^T \left(\sum_{i=1}^n \alpha_i b_i(x) \right) \quad (154)$$

$$= v^T f(x) \quad (155)$$

■

Proposition 6 (Riesz Representation) *Let \mathbb{H} be a vector valued RKHS taking a set \mathcal{X} to \mathbb{R}^d , and l be a **bounded** linear functional taking \mathbb{H} to \mathbb{R} then there is a unique $l^* \in \mathbb{H}$ for which for any $h \in \mathbb{H}$*

$$l(h) = \langle h, l^* \rangle_{\mathbb{H}}$$

Where $\langle \cdot, * \rangle_{\mathbb{H}}$ is the inner product in \mathbb{H} . Moreover l^* is given by

$$l^*(x) = \sum_{i=1}^d l(K_{\mathbb{H}}(\cdot, x)e_i) e_i$$

Where $K_{\mathbb{H}}(\cdot, *)$ is the reproducing kernel for the RKHS.

Proof Existence and uniqueness is guaranteed by Riesz representation theorem. To derive the form of l^* let $w \in \mathbb{R}^d$ and $x \in \mathcal{X}$ be arbitrary and consider (using the reproducing property of vector valued RKHSs)

$$w^T l^*(x) = \langle l^*, K_{\mathbb{H}}(\cdot, x)w \rangle_{\mathbb{H}} \quad (156a)$$

$$= \langle K_{\mathbb{H}}(\cdot, x)w, l^* \rangle_{\mathbb{H}} \quad (156b)$$

$$= l(K_{\mathbb{H}}(\cdot, x)w) \quad (156c)$$

$$= l(K_{\mathbb{H}}(\cdot, x)I_d w) \quad (156d)$$

$$= l\left(K_{\mathbb{H}}(\cdot, x) \left(\sum_{i=1}^d e_i e_i^T\right) w\right) \quad (156e)$$

$$= l\left(\sum_{i=1}^d K_{\mathbb{H}}(\cdot, x)e_i (e_i^T w)\right) \quad (156f)$$

$$= \sum_{i=1}^d l(K_{\mathbb{H}}(\cdot, x)e_i) e_i^T w \quad (156g)$$

$$= \sum_{i=1}^d w^T e_i l(K_{\mathbb{H}}(\cdot, x)e_i) \quad (156h)$$

$$= w^T \left(\sum_{i=1}^d l(K_{\mathbb{H}}(\cdot, x)e_i) e_i\right) \quad (156i)$$

Where we use the reproducing property, symmetry of real inner product, the definition of l^* , a clever form of multiplying by an identity, and linearity of the linear functional. Notice, in order to move the sum outside the linear functional, we also require $K_{\mathbb{H}}(\cdot, x)e_i \in \mathbb{H}$ which holds by the definition of vvRKHS's. Since w and x were chosen arbitrarily, we may conclude that

$$l^*(x) = \sum_{i=1}^d l(K_{\mathbb{H}}(\cdot, x)e_i) e_i$$

■

Theorem 7 (Existence and Uniqueness) Let $\mathbb{H}, \mathbb{V}_1, \dots, \mathbb{V}_n$ be vector valued RKHSs with kernels

$$K_{\mathbb{H}}, K_{\mathbb{V}_1}, \dots, K_{\mathbb{V}_n},$$

inner products

$$\langle \cdot, * \rangle_{\mathbb{H}}, \langle \cdot, * \rangle_{\mathbb{V}_1}, \dots, \langle \cdot, * \rangle_{\mathbb{V}_n}$$

and norms

$$\|\cdot\|_{\mathbb{H}}, \|\cdot\|_{\mathbb{V}_1}, \dots, \|\cdot\|_{\mathbb{V}_n}$$

respectively. Assume \mathbb{H} takes a set \mathcal{X} to \mathbb{R}^d and \mathbb{V}_i takes a set \mathcal{Y}_i to \mathbb{R}^{d_i} . Assume also $\mathbb{V}_1, \dots, \mathbb{V}_n$ are finite dimensional with dimensions q_1, \dots, q_n and feature functions Ψ_1, \dots, Ψ_n with $\Psi_i : \mathcal{Y}_i \Rightarrow \mathbb{R}^{q_i \times d_i}$ respectively. Let p_1, \dots, p_n be bilinear functionals taking $\mathbb{H} \times \mathbb{V}_i$ to \mathbb{R} that are continuous with respect to both entries. That is to say, for a fixed $v \in \mathbb{V}_i$, There is a constant K_v such that for any $h \in \mathbb{H}$.

$$|p_i(h, v)| \leq K_v \|h\|_{\mathbb{H}} \quad (157)$$

and for any fixed $h \in \mathbb{H}$ there is a constant K_h such that for any $v \in \mathbb{V}_i$

$$|p_i(h, v)| \leq K_h \|v\|_{\mathbb{V}_i} \quad (158)$$

Let l_1, \dots, l_n be continuous linear functionals taking $\mathbb{V}_1, \dots, \mathbb{V}_n$ to \mathbb{R} so that there is a constant K_i such that for any $v \in \mathbb{V}_i$,

$$|l_i(v)| \leq K_i \|v\|_{\mathbb{V}_i} \quad (159)$$

(Note, since \mathbb{V}_i are finite dimensional all linear functionals taking \mathbb{V}_i to \mathbb{R} are bounded) then for any strictly increasing function $\lambda : [0, \infty) \rightarrow [0, \infty)$ there is a unique solution to the variational problem:

$$\inf_{f \in \mathbb{H}} \left\{ \sum_{i=1}^n \sup_{\{v \in \mathbb{V}_i \mid \|v\|=1\}} \left\{ (p_i(f, v) - l_i(v))^2 \right\} + \lambda(\|f\|_{\mathbb{H}}^2) \right\} \quad (160)$$

Moreover, assuming $\lambda(\|x\|_{\mathbb{H}}^2) = \lambda \cdot \|x\|_{\mathbb{H}}^2, \lambda > 0$ (is the quadratic function) this unique solution is given by solving the linear system

$$(M + \lambda I) \alpha = y \quad (161)$$

with $f(x) \in \mathbb{H}$ given by

$$f(x) = \sum_{i=1}^n \sum_{k=1}^{q_i} \alpha_{i,k} \mathcal{L}_{i,k}^*(x) \quad (162)$$

$$\mathcal{L}_{i,k}^*(*) = \sum_{j=1}^d p_i(K_{\mathbb{H}}(\cdot, *) e_j, \Psi_i(\cdot)^T e_k) e_j \quad (163)$$

Letting $N = \sum_{i=1}^n q_i$, $M \in \mathbb{R}^{N \times N}$ is given by

$$M_{l,m;i,k} = \langle \mathcal{L}_{l,m}^*, \mathcal{L}_{i,k}^* \rangle_{\mathbb{H}} \quad (164)$$

so that

$$M = \begin{bmatrix} M_{1,1} & \dots & M_{1,n} \\ \vdots & \ddots & \vdots \\ M_{n,1} & \dots & M_{n,n} \end{bmatrix}$$

where the i, j th block is the matrix:

$$M_{i:j} = \begin{bmatrix} M_{i,1:j,1} & \dots & M_{i,1:j,q_j} \\ \vdots & \ddots & \vdots \\ M_{i,q_i:j,1} & \dots & M_{i,q_i:j,q_j} \end{bmatrix}$$

with

$$M_{l,m,i,k} = \langle \mathcal{L}_{l,m}^*, \mathcal{L}_{i,k}^* \rangle_{\mathbb{H}} = p_i \left(\sum_{j=1}^d p_l (K_{\mathbb{H}}(\cdot, *) e_j, \Psi_l(\cdot)^T e_m) e_j, \Psi_i(\cdot)^T e_k \right) \quad (165)$$

and y is given by

$$y_{i,k} = l_i(\Psi_i(\cdot)^T e_k) \quad (166)$$

so that

$$y = \begin{bmatrix} y_{1,1} \\ \vdots \\ y_{1,q_1} \\ y_{2,1} \\ \vdots \\ y_{2,q_2} \\ \vdots \\ y_{n,q_n} \end{bmatrix} \quad (167)$$

Proof We break this proof up into three separate parts. In part one, we simplify and evaluate the supremum, in part two we evaluate the inner products in terms of the linear functionals and bilinear forms, and in the final part we demonstrate a representer theorem argument to arrive at our final conclusion.

Part 1: Fix f and consider

$$\sup_{\{v \in \mathbb{V}_i \mid \|v\|_{\mathbb{V}_i} = 1\}} \left\{ (p_i(f, v) - l_i(v))^2 \right\} \quad (168)$$

Since p_i and l_i are bounded, we can apply theorem 3 to rewrite the interior of the supremum as

$$(p_i(f, v) - l_i(v))^2 = \left(\langle v, \mathcal{L}_{i,f}^* \rangle_{\mathbb{V}_i} - \langle v, l_i^* \rangle_{\mathbb{V}_i} \right)^2 \quad (169)$$

with $\mathcal{L}_{i,f}^* \in \mathbb{V}_i$ and $l_i^* \in \mathbb{V}_i$ given by

$$\mathcal{L}_{i,f}^*(*) = \sum_{j=1}^{d_i} p_i(f(\cdot), K_{\mathbb{V}_i}(\cdot, *) e_j) e_j \quad (170)$$

and

$$l_i^*(*) = \sum_{j=1}^{d_i} l_i(K_{\mathbb{V}_i}(\cdot, *) e_j) e_j \quad (171)$$

Now

$$\sup_{\{v \in \mathbb{V}_i \mid \|v\|_{\mathbb{V}_i} = 1\}} \left\{ \left(\langle v, \mathcal{L}_{i,f}^* - l_i^* \rangle_{\mathbb{V}_i} \right)^2 \right\} = \left(\left\langle \frac{\mathcal{L}_{i,f}^* - l_i^*}{\|\mathcal{L}_{i,f}^* - l_i^*\|_{\mathbb{V}_i}}, \mathcal{L}_{i,f}^* - l_i^* \right\rangle_{\mathbb{V}_i} \right)^2 \quad (172)$$

$$= \frac{\|\mathcal{L}_{i,f}^* - l_i^*\|_{\mathbb{V}_i}^4}{\|\mathcal{L}_{i,f}^* - l_i^*\|_{\mathbb{V}_i}^2} \quad (173)$$

$$= \|\mathcal{L}_{i,f}^* - l_i^*\|_{\mathbb{V}_i}^2 \quad (174)$$

$$= \langle \mathcal{L}_{i,f}^* - l_i^*, \mathcal{L}_{i,f}^* - l_i^* \rangle_{\mathbb{V}_i} \quad (175)$$

Therefore

$$(27) \Leftrightarrow \inf_{f \in \mathbb{H}} \left\{ \sum_{i=1}^n \left(\langle \mathcal{L}_{i,f}^* - l_i^*, \mathcal{L}_{i,f}^* - l_i^* \rangle_{\mathbb{V}_i} \right) + \lambda(\|f\|_{\mathbb{H}}^2) \right\} \quad (176)$$

Part 2: Notice, our inner products are real valued so $\langle l_i^*, \mathcal{L}_{i,f}^* \rangle_{\mathbb{V}_i} = \langle \mathcal{L}_{i,f}^*, l_i^* \rangle_{\mathbb{V}_i}$. Lets evaluate

$$\langle \mathcal{L}_{i,f}^*, \mathcal{L}_{i,f}^* \rangle_{\mathbb{V}_i}, \langle l_i^*, \mathcal{L}_{i,f}^* \rangle_{\mathbb{V}_i}, \langle l_i^*, l_i^* \rangle_{\mathbb{V}_i} \quad (177)$$

$$\langle l_i^*, l_i^* \rangle_{\mathbb{V}_i} = l_i(l_i^*(*)) \quad (178)$$

$$= l_i \left(\sum_{j=1}^{d_i} l_i(K_{\mathbb{V}_i}(\cdot, *)e_j)e_j \right) \quad (179)$$

Where the inside linear functional is taken over \cdot and the outside linear functional over $*$. Recall we define d_i to be the dimensionality of the range of the functions in \mathbb{V}_i . In addition, assuming $K_{\mathbb{V}_i}$ is finite dimensional of dimension q_i (i.e. with q_i features), so that

$$K_{\mathbb{V}_i}(\cdot, *) = \Psi_i(\cdot)^T \Psi_i(*) \in \mathbb{R}^{d_i \times d_i} \quad (180)$$

for some

$$\Psi_i : \mathcal{Y}_i \Rightarrow \mathbb{R}^{q_i \times d_i} \quad (181)$$

and assuming $e_k \in \text{span}\{\Psi_i(*)\alpha, \alpha \in \mathbb{R}^{d_i}, * \in \mathcal{X}\}$ for all k , we may further simplify as follows:

$$= l_i \left(\sum_{j=1}^{d_i} l_i(K_{\mathbb{V}_i}(\cdot, *)e_j)e_j \right) \quad (182)$$

$$= l_i \left(\sum_{j=1}^{d_i} l_i(\Psi_i(\cdot)^T \Psi_i(*)e_j)e_j \right) \quad (183)$$

$$= l_i \left(\sum_{j=1}^{d_i} l_i \left(\Psi_i(\cdot)^T \left(\sum_{k=1}^{q_i} e_k e_k^T \right) \Psi_i(*)e_j \right) e_j \right) \quad (184)$$

$$= l_i \left(\sum_{j=1}^{d_i} \sum_{k=1}^{q_i} l_i \left(\Psi_i(\cdot)^T (e_k e_k^T) \Psi_i(*)e_j \right) e_j \right) \quad (185)$$

$$= l_i \left(\sum_{j=1}^{d_i} \sum_{k=1}^{q_i} l_i \left(\Psi_i(\cdot)^T e_k \right) (e_k^T \Psi_i(*)e_j) e_j \right) \quad (186)$$

$$= l_i \left(\sum_{j=1}^{d_i} \sum_{k=1}^{q_i} l_i \left(\Psi_i(\cdot)^T e_k \right) e_j (e_j^T \Psi_i(*)^T e_k) \right) \quad (187)$$

$$= l_i \left(\sum_{k=1}^{q_i} l_i \left(\Psi_i(\cdot)^T e_k \right) \sum_{j=1}^{d_i} (e_j e_j^T) (\Psi_i(*)^T e_k) \right) \quad (188)$$

$$= l_i \left(\sum_{k=1}^{q_i} l_i \left(\Psi_i(\cdot)^T e_k \right) (\Psi_i(*)^T e_k) \right) \quad (189)$$

$$= \sum_{k=1}^{q_i} l_i \left(\Psi_i(\cdot)^T e_k \right) l_i \left(\Psi_i(*)^T e_k \right) \quad (190)$$

$$= \sum_{k=1}^{q_i} (l_i(\Psi(\cdot)^T e_k))^2 \quad (191)$$

Next let us evaluate

$$\langle l_i^*, \mathcal{L}_{i,f}^* \rangle_{\mathbb{V}_i} = \mathcal{L}_{i,f}(l_i^*(*)) \quad (192)$$

$$= \mathcal{L}_{i,f} \left(\sum_{j=1}^{d_i} l_i(K_{\mathbb{V}_i}(\cdot, *)e_j)e_j \right) \quad (193)$$

$$= \mathcal{L}_{i,f} \left(\sum_{j=1}^{d_i} l_i(\Psi_i(\cdot)^T \Psi_i(*)e_j)e_j \right) \quad (194)$$

$$= \mathcal{L}_{i,f} \left(\sum_{j=1}^{d_i} l_i \left(\Psi_i(\cdot)^T \left(\sum_{k=1}^{q_i} e_k e_k^T \right) \Psi_i(*)e_j \right) e_j \right) \quad (195)$$

$$= \mathcal{L}_{i,f} \left(\sum_{j=1}^{d_i} l_i \left(\Psi_i(\cdot)^T \left(\sum_{k=1}^{q_i} e_k e_k^T \right) \Psi_i(*)e_j \right) e_j \right) \quad (196)$$

$$= \mathcal{L}_{i,f} \left(\sum_{j=1}^{d_i} \sum_{k=1}^{q_i} l_i \left(\Psi_i(\cdot)^T e_k (e_k^T \Psi_i(*)e_j) \right) e_j \right) \quad (197)$$

$$= \mathcal{L}_{i,f} \left(\sum_{j=1}^{d_i} \sum_{k=1}^{q_i} l_i \left(\Psi_i(\cdot)^T e_k \right) (e_k^T \Psi_i(*)e_j) e_j \right) \quad (198)$$

$$= \mathcal{L}_{i,f} \left(\sum_{j=1}^{d_i} \sum_{k=1}^{q_i} l_i \left(\Psi_i(\cdot)^T e_k \right) e_j (e_j^T \Psi_i(*)^T e_k) \right) \quad (199)$$

$$= \mathcal{L}_{i,f} \left(\sum_{k=1}^{q_i} l_i \left(\Psi_i(\cdot)^T e_k \right) (\Psi_i(*)^T e_k) \right) \quad (200)$$

$$= \sum_{k=1}^{q_i} \mathcal{L}_{i,f} \left((\Psi_i(*)^T e_k) \right) l_i \left(\Psi_i(\cdot)^T e_k \right) \quad (201)$$

$$= \sum_{k=1}^{q_i} p_i \left(f(*), \Psi_i^T(*)e_k \right) l_i \left(\Psi_i(\cdot)^T e_k \right) \quad (202)$$

Finally,

$$\langle \mathcal{L}_{i,f}^*, \mathcal{L}_{i,f}^* \rangle_{\mathbb{V}_i} = \mathcal{L}_{i,f}(\mathcal{L}_{i,f}^*(*)) \quad (203)$$

$$= \mathcal{L}_{i,f} \left(\sum_{j=1}^{d_i} p_i(f(\cdot), K_{\mathbb{V}_i}(\cdot, *) e_j) e_j \right) \quad (204)$$

$$= \mathcal{L}_{i,f} \left(\sum_{j=1}^{d_i} p_i(f(\cdot), \Psi_i(\cdot)^T \Psi_i(*) e_j) e_j \right) \quad (205)$$

$$= \mathcal{L}_{i,f} \left(\sum_{j=1}^{d_i} p_i \left(f(\cdot), \Psi_i(\cdot)^T \left(\sum_{k=1}^{q_i} e_k e_k^T \right) \Psi_i(*) e_j \right) e_j \right) \quad (206)$$

$$= \mathcal{L}_{i,f} \left(\sum_{j=1}^{d_i} \sum_{k=1}^{q_i} p_i(f(\cdot), \Psi_i(\cdot)^T e_k) (e_k^T \Psi_i(*) e_j) e_j \right) \quad (207)$$

$$= \mathcal{L}_{i,f} \left(\sum_{j=1}^{d_i} \sum_{k=1}^{q_i} p_i(f(\cdot), \Psi_i(\cdot)^T e_k) e_j (e_j^T \Psi_i(*)^T e_k) \right) \quad (208)$$

$$= \mathcal{L}_{i,f} \left(\sum_{k=1}^{q_i} p_i(f(\cdot), \Psi_i(\cdot)^T e_k) (\Psi_i(*)^T e_k) \right) \quad (209)$$

$$= \sum_{k=1}^{q_i} (p_i(f(\cdot), \Psi_i(\cdot)^T e_k) \mathcal{L}_{i,f}(\Psi_i(*)^T e_k)) \quad (210)$$

$$= \sum_{k=1}^{q_i} (p_i(f(\cdot), \Psi_i(\cdot)^T e_k))^2 \quad (211)$$

Our loss is then

$$\inf_{f \in \mathbb{H}} \left\{ \sum_{i=1}^n \sum_{k=1}^{q_i} \left(p_i(f(*), \Psi_i^T(*) e_k)^2 - 2p_i(f(*), \Psi_i^T(*) e_k) l_i(\Psi_i(\cdot)^T e_k) \right. \right. \\ \left. \left. + (l_i(\Psi_i(\cdot)^T e_k))^2 + \lambda(\|f\|_{\mathbb{H}}^2) \right) \right\} \quad (212)$$

which is

$$\inf_{f \in \mathbb{H}} \left\{ \sum_{i=1}^n \sum_{k=1}^{q_i} (p_i(f(*), \Psi_i^T(*) e_k) - l_i(\Psi_i(*)^T e_k))^2 + \lambda(\|f\|_{\mathbb{H}}^2) \right\} \quad (213)$$

Part 3: Now we use theorem 3 once again, recalling that p_i is continuous with respect to f for any choice of v to rewrite the loss as

$$\inf_{f \in \mathbb{H}} \left\{ \sum_{i=1}^n \sum_{k=1}^{q_i} \left(\langle f, \mathcal{L}_{i,k}^* \rangle_{\mathbb{H}} - l_i(\Psi_i(*)^T e_k) \right)^2 + \lambda(\|f\|_{\mathbb{H}}^2) \right\} \quad (214)$$

where

$$\mathcal{L}_{i,k}^*(*) = \sum_{j=1}^d p_i(K_{\mathbb{H}}(\cdot, *) e_j, \Psi_i(\cdot)^T e_k) e_j \quad (215)$$

We may use a representer theorem argument to conclude that

$$f \in \text{span} \{ \mathcal{L}_{i,k}^* \} \quad (216)$$

Indeed, letting

$$f^* = \sum_{i=1}^n \sum_{k=1}^{q_i} \alpha_{i,k} \mathcal{L}_{i,k}^* \quad (217)$$

and

$$f = f^* + f^\perp \quad (218)$$

we get:

$$\inf_{f \in \mathbb{H}} \left\{ \sum_{i=1}^n \sum_{k=1}^{q_i} \left(\langle f, \mathcal{L}_{i,k}^* \rangle_{\mathbb{H}} - l_i(\Psi_i(\cdot)^T e_k) \right)^2 + \lambda(\|f\|_{\mathbb{H}}^2) \right\} \quad (219)$$

$$\Leftrightarrow \inf_{f \in \mathbb{H}} \left\{ \sum_{i=1}^n \sum_{k=1}^{q_i} \left(\langle f^* + f^\perp, \mathcal{L}_{i,k}^* \rangle_{\mathbb{H}} - l_i(\Psi_i(\cdot)^T e_k) \right)^2 + \lambda(\|f^* + f^\perp\|_{\mathbb{H}}^2) \right\} \quad (220)$$

$$\Leftrightarrow \inf_{f \in \mathbb{H}} \left\{ \sum_{i=1}^n \sum_{k=1}^{q_i} \left(\langle f^*, \mathcal{L}_{i,k}^* \rangle_{\mathbb{H}} - l_i(\Psi_i(\cdot)^T e_k) \right)^2 + \lambda(\|f^* + f^\perp\|_{\mathbb{H}}^2) \right\} \quad (221)$$

$$\geq \inf_{f^* \in \mathbb{H}} \left\{ \sum_{i=1}^n \sum_{k=1}^{q_i} \left(\langle f^*, \mathcal{L}_{i,k}^* \rangle_{\mathbb{H}} - l_i(\Psi_i(\cdot)^T e_k) \right)^2 + \lambda(\|f^*\|_{\mathbb{H}}^2) \right\} \quad (222)$$

$$(223)$$

If λ is a strictly increasing function we get a strict inequality and uniqueness of the solution. Thus we get the finite dimensional optimization problem

$$\inf_{\alpha_{l,m}} \left\{ \sum_{i=1}^n \sum_{k=1}^{q_i} \left(\sum_{l=1}^n \sum_{m=1}^{q_l} \alpha_{l,m} \langle \mathcal{L}_{l,m}^*, \mathcal{L}_{i,k}^* \rangle_{\mathbb{H}} - l_i(\Psi_i(\cdot)^T e_k) \right)^2 + \lambda \left(\sum_{l=1}^n \sum_{m=1}^{q_l} \sum_{i=1}^n \sum_{k=1}^{q_i} \alpha_{l,m} \alpha_{i,k} \langle \mathcal{L}_{l,m}^*, \mathcal{L}_{i,k}^* \rangle_{\mathbb{H}} \right) \right\} \quad (224)$$

Assuming $\lambda(\|f\|_{\mathbb{H}}^2) = \lambda\|f\|_{\mathbb{H}}^2$ and $N = \sum_{i=1}^n q_i$. Letting $M \in \mathbb{R}^{N \times N}$ with

$$M_{l,m,i,k} = \langle \mathcal{L}_{l,m}^*, \mathcal{L}_{i,k}^* \rangle_{\mathbb{H}} \quad (225)$$

$$\langle \mathcal{L}_{l,m}^*, \mathcal{L}_{i,k}^* \rangle_{\mathbb{H}} = \mathcal{L}_{i,k}(\mathcal{L}_{l,m}^*(\cdot)) \quad (226)$$

$$= \mathcal{L}_{i,k} \left(\sum_{j=1}^d p_l (K_{\mathbb{H}}(\cdot, *) e_j, \Psi_l(\cdot)^T e_m) e_j \right) \quad (227)$$

$$= \mathcal{L}_{i,k} \left(\sum_{j=1}^d p_l (K_{\mathbb{H}}(\cdot, *) e_j, \Psi_l(\cdot)^T e_m) e_j \right) \quad (228)$$

$$= p_i \left(\sum_{j=1}^d p_l (K_{\mathbb{H}}(\cdot, *) e_j, \Psi_l(\cdot)^T e_m) e_j, \Psi_i(\cdot)^T e_k \right) \quad (229)$$

$$(230)$$

Notice, unless we know the bilinear form is defined for functions of the form

$$p_l(K_{\mathbb{H}}(\cdot, *)e_j, \Psi_l(\cdot)^T e_m) \quad (231)$$

we can't pull the sum outside the bilinear form. In practice, after the bilinear form is defined we can move the sum outside. In all other cases, we are careful to only move the sum outside if the term on the inside is an element of the RKHS over which the linear functionals or bilinear functionals are defined. Letting $y \in \mathbb{R}^N$ with

$$y_{i,k} = l_i(\Psi_i(\cdot)^T e_k) \quad (232)$$

we get $\alpha \in \mathbb{R}^N$ by solving the linear system

$$(M + \lambda I) \alpha = y \quad (233)$$

■

Appendix B. Ridge Regression Example

Assuming we wish to minimize:

$$\min_{f \in \mathbb{H}} \left\{ \sum_{i=1}^n \|f(x_i) - y_i\|^2 + \|f\|_{\mathbb{H}}^2 \right\} \quad (234)$$

where \mathbb{H} is a vector valued RKHS with matrix valued kernel $K_{\mathbb{H}}(\cdot, *) \in \mathbb{R}^{p \times p}$. The standard ridge regression solution is

$$f(x) = [K_{\mathbb{H}}(x, x_1), \dots, K_{\mathbb{H}}(x, x_n)] \alpha \quad (235)$$

with

$$\alpha = (M + \lambda I)^{-1} Y \quad (236)$$

with

$$M = M^T = \begin{bmatrix} K_{\mathbb{H}}(x_1, x_1) & \dots & K_{\mathbb{H}}(x_1, x_n) \\ \vdots & \ddots & \vdots \\ K_{\mathbb{H}}(x_n, x_1) & \dots & K_{\mathbb{H}}(x_n, x_n) \end{bmatrix} \quad (237)$$

and

$$Y = \begin{bmatrix} y_1 \\ \vdots \\ y_n \end{bmatrix} \quad (238)$$

Treating the problem as a variational problem we minimize the loss:

$$\inf_{f \in \mathbb{H}} \left\{ \sum_{i=1}^n \sum_{j=1}^p \sup_{v \in \mathbb{V}_{i,j}, \|v\|=1} \{ (p_{i,j}(f, v) - l_{i,j}(v))^2 \} + \lambda \|f\|^2 \right\} \quad (239)$$

Where $\mathbb{V}_{i,j}$ is a vector valued RKHS with the (somewhat trivial) constant kernel $K(\cdot, *) = e_j e_j^T = \Psi_{i,j}(\cdot)^T \Psi_{i,j}(*)$ with $\Psi_{i,j}(\cdot) = e_j^T$.

$$p_{i,j}(f, v) = f(x_i)^T v(x_i) = f(x_i)^T e_j \quad (240)$$

and

$$l_{i,j}(v) = y_i^T v(x_i) = y_i^T e_j \quad (241)$$

7 allows us to conclude

$$f(x) = \sum_{i=1}^n \sum_{j=1}^p \sum_{k=1}^1 \alpha_{i,j,k} \mathcal{L}_{i,j,k}^*(x) \quad (242)$$

with k the dimension of the feature space (1 in our case) and

$$\mathcal{L}_{i,j,k}^*(*) = \sum_{l=1}^p P_{i,j} (K_{\mathbb{H}}(\cdot, *) e_l, \Psi_{i,j}(\cdot)^T e_k) e_l \quad (243)$$

Here $\Psi_{i,j}(\cdot)^T = e_j$ and $e_k = 1$ so we simplify to

$$\mathcal{L}_{i,j,k}^*(*) = \sum_{l=1}^p P_{i,j} (K_{\mathbb{H}}(\cdot, *) e_l, e_j) e_l \quad (244)$$

$$= \sum_{l=1}^p \left[(K_{\mathbb{H}}(x_i, *) e_l)^T e_j \right] e_l \quad (245)$$

$$= \sum_{l=1}^p [e_l^T K_{\mathbb{H}}(*, x_i) e_j] e_l \quad (246)$$

$$= \sum_{l=1}^p [e_l e_l^T K_{\mathbb{H}}(*, x_i) e_j] \quad (247)$$

$$= \left(\sum_{l=1}^p e_l e_l^T \right) K_{\mathbb{H}}(*, x_i) e_j \quad (248)$$

$$= K(*, x_i) e_j \quad (249)$$

Thus

$$f(*) = \sum_{i=1}^n \sum_{j=1}^p \alpha_{i,j} K_{\mathbb{H}}(*, x_i) e_j = \sum_{i=1}^n K_{\mathbb{H}}(*, x_i) \alpha_i \quad (250)$$

This proves f takes the form as in Regression, all that is left to prove is the α we learn is the same as that learned by Regression. For this, recall from 7 that the α we desire to learn satisfies

$$(M + \lambda I) \alpha = Y \quad (251)$$

Where

$$M = \begin{bmatrix} \langle \mathcal{L}_{1,1}^*, \mathcal{L}_{1,1}^* \rangle & \langle \mathcal{L}_{1,2}^*, \mathcal{L}_{1,1}^* \rangle & \cdots & \langle \mathcal{L}_{1,p}^*, \mathcal{L}_{1,1}^* \rangle & \langle \mathcal{L}_{2,1}^*, \mathcal{L}_{1,1}^* \rangle & \cdots & \langle \mathcal{L}_{n,p}^*, \mathcal{L}_{1,1}^* \rangle \\ \langle \mathcal{L}_{1,1}^*, \mathcal{L}_{1,2}^* \rangle & \langle \mathcal{L}_{1,2}^*, \mathcal{L}_{1,2}^* \rangle & \cdots & \langle \mathcal{L}_{1,p}^*, \mathcal{L}_{1,2}^* \rangle & \langle \mathcal{L}_{2,1}^*, \mathcal{L}_{1,2}^* \rangle & \cdots & \langle \mathcal{L}_{n,p}^*, \mathcal{L}_{1,2}^* \rangle \\ \vdots & \vdots & \ddots & \vdots & \vdots & \ddots & \vdots \\ \langle \mathcal{L}_{1,1}^*, \mathcal{L}_{1,p}^* \rangle & \langle \mathcal{L}_{1,2}^*, \mathcal{L}_{1,p}^* \rangle & \cdots & \langle \mathcal{L}_{1,p}^*, \mathcal{L}_{1,p}^* \rangle & \langle \mathcal{L}_{2,1}^*, \mathcal{L}_{1,p}^* \rangle & \cdots & \langle \mathcal{L}_{n,p}^*, \mathcal{L}_{1,p}^* \rangle \\ \langle \mathcal{L}_{1,1}^*, \mathcal{L}_{2,1}^* \rangle & \langle \mathcal{L}_{1,2}^*, \mathcal{L}_{2,1}^* \rangle & \cdots & \langle \mathcal{L}_{1,p}^*, \mathcal{L}_{2,1}^* \rangle & \langle \mathcal{L}_{2,1}^*, \mathcal{L}_{2,1}^* \rangle & \cdots & \langle \mathcal{L}_{n,p}^*, \mathcal{L}_{2,1}^* \rangle \\ \vdots & \vdots & \ddots & \vdots & \vdots & \ddots & \vdots \\ \langle \mathcal{L}_{1,1}^*, \mathcal{L}_{n,p}^* \rangle & \langle \mathcal{L}_{1,2}^*, \mathcal{L}_{n,p}^* \rangle & \cdots & \langle \mathcal{L}_{1,p}^*, \mathcal{L}_{n,p}^* \rangle & \langle \mathcal{L}_{2,1}^*, \mathcal{L}_{n,p}^* \rangle & \cdots & \langle \mathcal{L}_{n,p}^*, \mathcal{L}_{n,p}^* \rangle \end{bmatrix} \quad (252)$$

and

$$Y = \begin{bmatrix} l_{1,1}(\Psi_{1,1}(\cdot)^T) \\ l_{1,2}(\Psi_{1,2}(\cdot)^T) \\ \vdots \\ l_{n,d}(\Psi_{n,p}(\cdot)^T) \end{bmatrix} \quad (253)$$

Note, since the feature function is one dimensional $e_k = 1 \in \mathbb{R}$ simplifying matters. Starting with Y we observe:

$$l_{i,j}(\Psi_{i,j}(\cdot)^T) = l_{i,j}(e_j) = y_i^T e_j \quad (254)$$

Thus

$$Y = \begin{bmatrix} y_1 \\ \vdots \\ y_n \end{bmatrix} \quad (255)$$

as desired. Finally,

$$\langle \mathcal{L}_{i,j}^*, \mathcal{L}_{k,l}^* \rangle = p_{i,j} \left\{ \sum_{m=1}^p p_{k,l} (K_{\mathbb{H}}(\cdot, *) e_m, \Psi_{k,l}(\cdot)^T \cdot 1) e_m, \Psi_{i,j}(\cdot)^T \cdot 1 \right\} \quad (256)$$

$$= p_{i,j} \left\{ \sum_{m=1}^p p_{k,l} (K_{\mathbb{H}}(\cdot, *) e_m, e_l) e_m, e_j \right\} \quad (257)$$

$$= p_{i,j} \left\{ \sum_{m=1}^p [(K_{\mathbb{H}}(x_k, *) e_m)^T e_l] e_m, e_j \right\} \quad (258)$$

$$= p_{i,j} \left\{ \sum_{m=1}^p [e_m^T K_{\mathbb{H}}(*, x_k) e_l] e_m, e_j \right\} \quad (259)$$

$$= p_{i,j} \{ K_{\mathbb{H}}(*, x_k) e_l, e_j \} \quad (260)$$

$$= e_l^T K_{\mathbb{H}}(x_k, x_i) e_j \quad (261)$$

Thus, M is also of the desired form. We note that once again we use the fact that the feature function is one dimensional.

Appendix C. Liouville Operator Occupation Kernel generalization

$$\inf_{u \in U} \left\| \int_0^T \nabla_2 (k(\cdot, \gamma(t)))^T f(\gamma(t)) dt - \int_0^T \nabla_2 (k(\cdot, \gamma(t)))^T u(\gamma(t)) dt \right\|_{\mathbb{V}}^2 \Leftrightarrow \inf_{u \in U} \left\{ \sup_{v \in \mathbb{V}, \|v\|=1} \left\{ \left(\int_0^T \nabla (v(\gamma(t)))^T f(\gamma(t)) dt - \int_0^T \nabla (v(\gamma(t)))^T u(\gamma(t)) dt \right)^2 \right\} \right\} \quad (262)$$

Since

$$\int_0^T \nabla (v(\gamma(t)))^T f(\gamma(t)) dt \quad (263)$$

is a bounded bilinear functional with respect to v , and

$$\int_0^T \nabla (v(\gamma(t)))^T u(\gamma(t)) dt \quad (264)$$

is a bounded bilinear form with respect to v and u , reisz representer theorem gaurantees occupation kernel representeres of these linear functionals in \mathbb{V} . These may be derived as in 3. Consider:

$$l(v) \equiv \int_0^T \nabla (v(\gamma(t)))^T f(\gamma(t)) dt \quad (265)$$

We seek

$$l^*(x) \quad (266)$$

for which

$$\langle v, l^* \rangle = l(v) \quad (267)$$

for every v . Observe

$$l^*(x) = \langle l^*, k(\cdot, x) \rangle \quad (268)$$

$$= \langle k(\cdot, x), l^* \rangle \quad (269)$$

$$= l(k(\cdot, x)) \quad (270)$$

$$= \int_0^T \nabla_2 (k(x, \gamma(t)))^T f(\gamma(t)) dt \quad (271)$$

Similarly, letting

$$\mathcal{L}(v) = \int_0^T \nabla (v(\gamma(t))) u(\gamma(t)) dt \quad (272)$$

we get

$$\mathcal{L}^*(x) = \int_0^T \nabla_2 (k(x, \gamma(t)))^T u(\gamma(t)) dt \quad (273)$$

and we rewrite the supremum as

$$\sup_{v \in \mathbb{V}, \|v\|=1} \left\{ \left(\int_0^T \nabla(v(\gamma(t)))^T f(\gamma(t)) dt - \int_0^T \nabla(v(\gamma(t)))^T u(\gamma(t)) dt \right)^2 \right\} \quad (274)$$

$$= \sup_{v \in \mathbb{V}, \|v\|=1} \left\{ \left(\left\langle v, \int_0^T \nabla_2(k(\cdot, \gamma(t)))^T f(\gamma(t)) dt - \int_0^T \nabla_2(k(\cdot, \gamma(t)))^T u(\gamma(t)) dt \right\rangle \right)^2 \right\} \quad (275)$$

$$= \left\| \int_0^T \nabla_2(k(\cdot, \gamma(t)))^T f(\gamma(t)) dt - \int_0^T \nabla_2(k(\cdot, \gamma(t)))^T u(\gamma(t)) dt \right\|_{\mathbb{V}}^2 \quad (276)$$

Appendix D. Weak formulation for the quasilinear PDE

D.1 Weak formulation minimization

To further motivate our approach, we present another example of a weak formulation derivation to a different type of problem altogether, the inverse problem of learning a PDE. Consider the PDE

$$\alpha(x)u_x + u_y = f(u) \quad (277)$$

Let \mathbb{G} be an RKHS of test functions with associated kernel function $G(\cdot, \cdot) : \mathbb{R}^2 \times \mathbb{R}^2 \rightarrow \mathbb{R}$. Let Ω be a compact set in \mathbb{R}^2 . From now on, we will assume that $u \in C^1(\Omega)$, $x \rightarrow f(x)$ and $x \rightarrow \alpha(x)$ are continuous. Define:

$$D_{f,\alpha}(x, y) := \alpha(x)u_x(x, y) + u_y(x, y) - f(u(x, y)) \quad (278)$$

and define

$$Q(f, \alpha) = \sup_{\Phi \in \mathbb{G}, \|\Phi\|=1} \left(\int_{\Omega} D_{f,\alpha}(x, y) \Phi(x, y) dx dy \right)^2 \quad (279)$$

Notice that the linear functional:

$$L_{f,\alpha}(\Phi) := \int_{\Omega} D_{f,\alpha}(x, y) \Phi(x, y) dx dy \quad (280)$$

is bounded with a norm bounded by

$$\int_{\Omega} |D_{f,\alpha}(x, y)| \sqrt{G((x, y), (x, y))} dx dy \quad (281)$$

and therefore is continuous. Hence, there exists a function $L_{f,\alpha}^* \in \mathbb{G}$ such that:

$$L_{f,\alpha}(\Phi) = \langle L_{f,\alpha}^*, \Phi \rangle \quad (282)$$

and

$$L_{f,\alpha}^*(u, v) = \int_{\Omega} D_{f,\alpha}(x, y) G((x, y), (u, v)) dx dy \quad (283)$$

Using Cauchy-Schwartz inequality, we conclude that:

$$Q(f, \alpha) = \|L_{f,\alpha}^*(u, v)\|^2 = \int_{\Omega \times \Omega} D_{f,\alpha}(x_1, y_1) D_{f,\alpha}(x_2, y_2) G((x_1, y_1), (x_2, y_2)) dx_1 dy_1 dx_2 dy_2 \quad (284)$$

It should be noted that if G is an explicit kernel, then just as in the case with ODEs, this term simplifies. Assume $G((x_1, y_2), (x_2, y_2)) = \phi(x_1, y_1)^T \phi(x_2, y_2)$ where $\phi : \mathbb{R}^2 \rightarrow \mathbb{R}^{nm}$. Then

$$Q(f, \alpha) = \left\| \int_{\Omega} (\alpha(x)u_x + u_y - f(u))\phi(x, y)dxdy \right\|_{\mathbb{R}^{nm}}^2 \quad (285)$$

D.2 Weak formulation minimization numerical solution

Assuming \mathbb{H}_1 and \mathbb{H}_2 are two RKHSs with kernels k_1 and k_2 respectively, We minimize:

$$\min_{\alpha \in \mathbb{H}_1, f \in \mathbb{H}_2} \{J(f, \alpha) = Q(f, \alpha) + \lambda_1 \|\alpha\|^2 + \lambda_2 \|f\|^2\} \quad (286)$$

assuming:

$$\phi_{i,j}(x, y) = \begin{cases} 1 & (x, y) \in [x_i, x_{i+1}] \times [y_j, y_{j+1}] \\ 0 & \text{otherwise} \end{cases} \quad (287)$$

as follows:

$$J(f, \alpha) = \sum_{i,j} \left(\int_{\Omega} (\alpha(x)u_x + u_y - f(u))\phi_{i,j}dxdy \right)^2 + \lambda_1 \|\alpha\|^2 + \lambda_2 \|f\|^2 \quad (288)$$

$$= \sum_{i,j} \left(\int_{x_i}^{x_{i+1}} \int_{y_j}^{y_{j+1}} (\alpha(x)u_x + u_y - f(u))dxdy \right)^2 + \lambda_1 \|\alpha\|^2 + \lambda_2 \|f\|^2 \quad (289)$$

We use the trapezoid rule and fundamental theorem of calculus to estimate the integral:

$$\int_{x_i}^{x_{i+1}} \int_{y_j}^{y_{j+1}} u_y dxdy \approx \frac{h}{2} (u(x_i, y_{j+1}) + u(x_{i+1}, y_{j+1}) - u(x_i, y_j) - u(x_{i+1}, y_j)) \equiv z_{i,j} \quad (290)$$

and we observe

$$\mathcal{L}_{i,j,u}(\alpha) \equiv \int_{x_i}^{x_{i+1}} \int_{y_j}^{y_{j+1}} \alpha(x)u_x dxdy \quad (291)$$

is a linear functional of α . Similarly

$$\mathcal{M}_{i,j,u}(f) \equiv \int_{x_i}^{x_{i+1}} \int_{y_j}^{y_{j+1}} f(u)dxdy \quad (292)$$

is a linear functional of f .

Since u_x is continuous, and assuming that the kernels k_1 and k_2 continuous we demonstrate that these linear functionals are bounded:

$$|\mathcal{L}_{i,j,u}(\alpha)|^2 = \left| \int_{x_i}^{x_{i+1}} \int_{y_j}^{y_{j+1}} \alpha(x) u_x dx dy \right|^2 \quad (293)$$

$$\leq \int_{x_i}^{x_{i+1}} \int_{y_j}^{y_{j+1}} (\alpha(x))^2 dx dy \int_{x_i}^{x_{i+1}} \int_{y_j}^{y_{j+1}} u_x^2 dx dy \quad (294)$$

$$\leq C_1 \int_{x_i}^{x_{i+1}} \int_{y_j}^{y_{j+1}} (\alpha(x))^2 dx dy \quad (295)$$

$$= C_1 \int_{x_i}^{x_{i+1}} \int_{y_j}^{y_{j+1}} (\langle \alpha, k_1(\cdot, x) \rangle)^2 dx dy \quad (296)$$

$$= C_1 \int_{x_i}^{x_{i+1}} \int_{y_j}^{y_{j+1}} \|\alpha\|^2 \|k_1(\cdot, x)\|^2 dx dy \quad (297)$$

$$= C_1 \|\alpha\|^2 \sup_u \|k_1(\cdot, u)\|^2 \int_{x_i}^{x_{i+1}} \int_{y_j}^{y_{j+1}} dx dy \quad (298)$$

$$\leq C \|\alpha\|^2 \quad (299)$$

Similarly,

$$|\mathcal{M}_{i,j,u}(f)|^2 = \left| \int_{x_i}^{x_{i+1}} \int_{y_j}^{y_{j+1}} f(u) dx dy \right|^2 \quad (300)$$

$$= \left| \int_{x_i}^{x_{i+1}} \int_{y_j}^{y_{j+1}} \langle f, k_2(\cdot, u) \rangle dx dy \right|^2 \quad (301)$$

$$= \left| \left\langle f, \int_{x_i}^{x_{i+1}} \int_{y_j}^{y_{j+1}} k_2(\cdot, u) dx dy \right\rangle \right|^2 \quad (302)$$

$$\leq \|f\|^2 \left\| \int_{x_i}^{x_{i+1}} \int_{y_j}^{y_{j+1}} k_2(\cdot, u) dx dy \right\|^2 \quad (303)$$

$$\leq C_2 \|f\|^2 \quad (304)$$

Therefore, there exist elements $L_{i,j,u}^* \in \mathbb{H}_1$ and $M_{i,j,u}^* \in \mathbb{H}_2$ respectively for which

$$\mathcal{M}_{i,j,u}(f) = \langle f, M_{i,j,u}^* \rangle, \quad \mathcal{L}_{i,j,u}(\alpha) = \langle \alpha, L_{i,j,u}^* \rangle \quad (305)$$

and

$$J(f, \alpha) = \sum_{i,j} (\langle \alpha, \mathcal{L}_{i,j,u}^* \rangle - \langle f, \mathcal{M}_{i,j,u}^* \rangle + z_{i,j})^2 + \lambda_1 \|\alpha\|^2 + \lambda_2 \|f\|^2 \quad (306)$$

Finally, we use the representer theorem for α and f to conclude that the minimizer of J with respect to f and α may be found in the span of $\mathcal{M}_{i,j,u}^*$ and $\mathcal{L}_{i,j,u}^*$ respectively. Thus, this is a linear regression problem with the solution:

$$\alpha(s) = \sum_{i,j} \alpha_{i,j} \mathcal{L}_{i,j,u}^*(s) \quad (307)$$

$$\mathcal{L}_{i,j,u}^*(s) = \int_{x_i}^{x_{i+1}} \int_{y_j}^{y_{j+1}} k_1(s, x) u_x dx dy \quad (308)$$

$$f(z) = \sum_{i,j} \beta_{i,j} M_{i,j,u}^*(z) \quad (309)$$

where

$$M_{i,j}^*(z) = \int_{x_i}^{x_{i+1}} \int_{y_j}^{y_{j+1}} k_2(z, u(x, y)) dx dy \quad (310)$$

and

$$y_{i,j} = \int_{x_i}^{x_{i+1}} \int_{y_j}^{y_{j+1}} u_y dx dy. \quad (311)$$

Finally, the coefficients $\alpha, \beta \in \mathbb{R}^{nm}$ are found by minimizing:

$$C(\alpha, \beta) := \|L\alpha - M\beta + y\|^2 + \lambda_1 \alpha^T L\alpha + \lambda_2 \beta^T M\beta \quad (312)$$

With $M, L \in \mathbb{R}^{nm \times nm}$ defined by:

$$L_{i,j,k,l} = \int_{x_i}^{x_{i+1}} \int_{y_j}^{y_{j+1}} \int_{x_k}^{x_{k+1}} \int_{y_l}^{y_{l+1}} k_1(s, x) u_s u_x ds dz dx dy \quad (313)$$

$$M_{i,j,k,l} = \int_{x_i}^{x_{i+1}} \int_{y_j}^{y_{j+1}} \int_{x_k}^{x_{k+1}} \int_{y_l}^{y_{l+1}} k_2(u(s, z), u(x, y)) ds dz dx dy \quad (314)$$

D.3 Numerical minimization with Explicit Kernels

Let us assume $k_1(x, y) = \psi_1(x)^T \psi_1(y)$ and $k_2(u, z) = \psi_2(u)^T \psi_2(z)$ with $\psi_1(x) \in \mathbb{R}^{p_1}$ and $\psi_2(x) \in \mathbb{R}^{p_2}$ then,

$$\alpha(s) = \sum_{i,j} \alpha_{i,j} \int_{x_i}^{x_{i+1}} \int_{y_j}^{y_{j+1}} \psi_1(s)^T \psi_1(x) u_x dx dy \quad (315)$$

$$= \psi_1(s)^T \left(\sum_{i,j} \alpha_{i,j} \int_{x_i}^{x_{i+1}} \int_{y_j}^{y_{j+1}} \psi_1(x) u_x dx dy \right) \quad (316)$$

$$(317)$$

and

$$f(z) = \sum_{i,j} \beta_{i,j} \int_{x_i}^{x_{i+1}} \int_{y_j}^{y_{j+1}} \psi_2(z)^T \psi_2(u) dx dy \quad (318)$$

$$= \psi_2(z)^T \left(\sum_{i,j} \beta_{i,j} \int_{x_i}^{x_{i+1}} \int_{y_j}^{y_{j+1}} \psi_2(u) dx dy \right) \quad (319)$$

We may define:

$$\gamma \equiv \sum_{i,j} \alpha_{i,j} \int_{x_i}^{x_{i+1}} \int_{y_j}^{y_{j+1}} \psi_1(x) u_x dx dy \quad (320)$$

$$\delta \equiv \sum_{i,j} \beta_{i,j} \int_{x_i}^{x_{i+1}} \int_{y_j}^{y_{j+1}} \psi_2(u) dx dy \quad (321)$$

Then

$$\alpha(s) = \psi_2(s)^T \gamma \quad (322)$$

$$f(z) = \psi_2(z)^T \delta \quad (323)$$

Defining $\Psi_1 \in \mathbb{R}^{p_1 \times nm}$ and $\Psi_2 \in \mathbb{R}^{p_2 \times nm}$ with

$$(\Psi_1)_{i,j} = \int_{x_i}^{x_{i+1}} \int_{y_j}^{y_{j+1}} \psi_1(x) u_x dx dy \in \mathbb{R}^{p_1} \quad (324)$$

and

$$(\Psi_2)_{i,j} = \int_{x_i}^{x_{i+1}} \int_{y_j}^{y_{j+1}} \psi_2(u) dx dy \in \mathbb{R}^{p_2} \quad (325)$$

Then we see

$$L = \Psi_1^T \Psi_1 \quad (326)$$

$$M = \Psi_2^T \Psi_2 \quad (327)$$

$$\gamma = \Psi_1 \alpha \quad (328)$$

and

$$\delta = \Psi_2 \beta \quad (329)$$

With this, we may rewrite 312 as:

$$C(\gamma, \delta) = \|\Psi_1^T \gamma - \Psi_2^T \delta + y\|^2 + \lambda_1 \gamma^T \gamma + \lambda_2 \delta^T \delta \quad (330)$$

Appendix E. Datasets

Appendix F. Experiments with the quasilinear PDE

In our experiments, we use an explicit kernel for k_1 and k_2 given by 100 random Fourier features for each of α and f . This allows us to simplify the regression problem (312) to a 200-dimensional one. Although the number of random Fourier features was fixed in all experiments, the error decreased roughly in proportion to the inverse of the total number of samples (as can be seen by the slope of the plot in figure 1). Our method allows us to solve the problem in a fixed-size solution space. Plots of $f(u(x, y))$ and $\alpha(x)$ and their errors are presented in Figure 1. This indicates that the main source of error is the quadrature estimation and not the weakness of the solution space.

Appendix G. ROCK Implementation

We employ some vectorization techniques to arrive at a remarkably concise and yet very general implementation of the ROCK method as follows: We note that theorem 7 requires us to evaluate

$$Y, \text{ and } M \quad (331)$$

n	m	α -error	f -error
100	10	21%	29%
200	20	4%	3.5%
400	40	.9%	.8%
800	80	.2%	.2%
1600	160	.06%	.05%
3200	320	.01%	.01%
6400	640	.003%	.003%
12800	1280	.0009%	.0008%

Table 11: Estimation errors for α and f (reported as percent error of α and f measured on the grid points). Although we fix the number of Fourier random features to 100 for alpha and 100 for f in all experiments, we see the error still decreases in proportion to the inverse of nm (the total number of samples) as n , and m increase. Where n is the number of samples taken across x and m is the number of samples across y in the grid. This suggests that errors may be improved with more data even as we fix the size of the solution space. This is in contrast to finite element methods which typically see the solution space grow with the number of samples. It also suggests we may see faster convergence if we use a higher order quadrature in the integration. For this demonstration we simply stick to the trapezoid rule to compute our integrals.

from which we calculate

$$\alpha \tag{332}$$

At which point we may evaluate f at new datapoints. For the following we assume the n th trajectory has m_i samples for us to use in our integral estimate. Recall:

$$Y \in \mathbb{R}^{pdn} \tag{333}$$

where for $i \in [1, \dots, n]$ and $j \in [1, \dots, p]$

$$y_{i,j} = x_i(b_i)[\psi_i(b_i)]_j - x_i(a_i)[\psi_i(a_i)]_j - \int_{a_i}^{b_i} x_i(t)[\dot{\psi}_i(t)]_j dt \in \mathbb{R}^d \tag{334}$$

here, $[\psi_i(b_i)]_j$ and $[\dot{\psi}_i(t)]_j$ are scalar valued, and $x_i(t) \in \mathbb{R}^d$. We calculate $\Psi \in \mathbb{R}^{np \times (\sum_{i=1}^n m_i)}$ a block diagonal matrix of test function evaluations with the blocks:

$$\psi_{i,i} = [\psi_i(t_1^i), \psi_i(t_2^i), \dots, \psi_i(t_{m_i}^i)] \in \mathbb{R}^{p \times m_i} \tag{335}$$

We calculate Ψ in a for loop through each of the n trajectories. This is the only part of the algorithm that is not fully vectorized, however, we choose to implement this in this way to allow for the freedom of using different test functions for each trajectory. We find this part of the algorithm to be insignificant in terms of runtime and memory costs. Each block is calculated in a vectorized way with the following python code. (We implement legendre polynomials over arbitrary intervals as our test functions as described in a previous section).

```

# We will be using Scaled and Shifted Legendre Polynomials
# ts - The array of times to evaluate the legendre polynomials at
# n - the order of the polynomial (integer with 0 <= n).
# a - The left end of the interval to shift the polynomials to
# b - the right end of the interval to shift the polynomials to. (b > a)
# Computes the Legendre Polynomials based on the recursion:
# P_{n+1}(x) = [(2n+1)xP_n(x) - nP_{n-1}(x)]/(n+1)
def phis(ts,n,a,b):
    # Apply the transformation of ts to tsp (on the interval [-1,1])
    if n == 0:
        Ts = np.ones((len(ts),1))
        return Ts
    tsp = (2/(b-a))*ts - (b+a)/(b-a)
    Ts = np.ones((len(ts),n+1))
    Ts[:,1] = tsp
    for i in range(2,n+1):
        Ts[:,i] = ((2*(i-1)+1)*tsp*Ts[:,i-1] - (i-1)*Ts[:,i-2])/(i)
    # The normalization term for the scaled Legendre Polynomial is
    # sqrt((2*n+1)/2)*sqrt(2/(b-a))
    Ts = Ts*np.sqrt((np.array(range(n+1))*2+1)/2)[None,:]*np.sqrt(2/(b-a))
    return Ts

```

In addition, we compute $\dot{\Psi}_{i,i} \in \mathbb{R}^{p \times m_i}$, a matrix of derivatives of the test functions. Code for calculating both $\Psi_{i,i}$ and $\dot{\Psi}_{i,i}$ in one function is presented below:

```

# We will be using Scaled and Shifted Legendre Polynomials
# We need the derivatives as well.
# ts - The array of times to evaluate the legendre polynomials at
# n - the order of the polynomial (integer with 0 <= n).
# a - The left end of the interval to shift the polynomials to
# b - the right end of the interval to shift the polynomials to. (b > a)
# Computes the derivative of the Legendre Polynomials based on the recursion
# :
# P_{n+1}(x) = [(2n+1)xP_n(x) - nP_{n-1}(x)]/(n+1), which implies:
# P'_{n+1}(x) = [(2n+1)P_n(x) + (2n+1)xP'_n(x) - nP'_{n-1}(x)]/(n+1)
def phisp(ts,n,a,b):
    # Apply the transformation of ts to tsp (on the interval [-1,1])
    tsp = (2/(b-a))*ts - (b+a)/(b-a)
    if n == 0:
        return np.ones((len(ts),1)), np.zeros((len(ts),1))
    Ts = np.ones((len(ts),n+1))
    Tsp = np.zeros((len(ts),n+1))
    Ts[:,1] = tsp
    Tsp[:,1] = 1
    for i in range(2,n+1):
        Ts[:,i] = ((2*(i-1)+1)*tsp*Ts[:,i-1] - (i-1)*Ts[:,i-2])/(i)
        Tsp[:,i] = ((2*(i-1)+1)*Ts[:,i-1] + (2*(i-1)+1)*tsp*Tsp[:,i-1] - (i-1)*Tsp[:,i-2])/(i)
    # The normalization term for the scaled Legendre Polynomial is
    # sqrt((2*n+1)/2)*sqrt(2/(b-a))
    Ts = Ts*np.sqrt((np.array(range(n+1))*2+1)/2)[None,:]*np.sqrt(2/(b-a))
    Tsp = Tsp*np.sqrt((np.array(range(n+1))*2+1)/2)[None,:]*np.sqrt(2/(b-a))*(
        2/(b-a))
    return Ts, Tsp

```

We construct $QPhi \in \mathbb{R}^{pn \times (\sum_{i=1}^n m_i)}$ and $QPhiD \in \mathbb{R}^{pn \times (\sum_{i=1}^n m_i)}$. These are both block diagonal matrices with the blocks:

$$QPhi_{i,i} = [q_1^i \Psi_i(t_1^i), q_2^i \Psi_i(t_2^i), \dots, q_{m_i}^i \Psi_i(t_{m_i}^i)] \in \mathbb{R}^{p \times m_i} \quad (336)$$

where q_j^i is the quadrature weight used to estimate the integral using the time points $t_1^i, \dots, t_{m_i}^i$. For instance, assuming $t_j^i = jh$, and using a composite trapezoid rule, $q_1^i = h/2$, $q_2^i = \dots = q_{m_i-1}^i = h$, $q_{m_i}^i = h/2$.

$$QPhiD_{i,i} = [-\Psi_i(t_1^i) - q_1^i \dot{\Psi}_i(t_1^i), -q_2^i \dot{\Psi}_i(t_2^i), \dots, -q_{m_i-1}^i \dot{\Psi}_i(t_{m_i-1}^i), \Psi_i(t_{m_i}^i) - q_{m_i}^i \dot{\Psi}_i(t_{m_i}^i)] \in \mathbb{R}^{p \times m_i} \quad (337)$$

Here we notice that in addition to the derivative terms, $QPhiD$ also involves the boundary terms on the first and last columns of each block. These block diagonal matrices are constructed in the following code (which contains the only for loop in the algorithm implementation).

```
# Requires a list of ts a list of qs, and outputs a block diagonal matrix
# corresponding to the QPhi block diagonal matrix and QPhiD block diagonal
# matrix.
# Probably the least efficient part of the code. (loops through the
# trajectories)

def Calculate_QPhi(qs,ts,n):
    psArr = []
    pspArr = []
    for i in range(len(ts)):
        ps, psp = phisp(ts[i],n,ts[i][0],ts[i][-1])
        psp = -(psp[:]*qs[i][:],None)
        # Add boundary terms to psp
        psp[0,:] = psp[0,:]-ps[0,:]
        psp[-1,:] = psp[-1,:]+ps[-1,:]
        psp = psp.T
        ps = (ps*qs[i][:],None).T
        psArr.append(ps)
        pspArr.append(psp)
    return sp.block_diag(psArr), sp.block_diag(pspArr)
```

Assuming $dataX \in \mathbb{R}^{d \times (\sum_{i=1}^n m_i)}$ is the dataset with trajectory i given by:

$$[x_i(t_1^i), \dots, x_i(t_{m_i}^i)] = dataX \left[:, \left(\sum_{k=1}^{i-1} m_k : \sum_{k=1}^i m_k \right) \right] \quad (338)$$

Then we may calculate Y with: $Y = dataX \cdot QPhiD^T \in \mathbb{R}^{d \times np}$ where \cdot is matrix matrix multiplication.

```
# Calculate Y, requires QPhi, QPhiD (derivatives of QPhi), data, and qs (to
# recover
# Phi from QPhi)
def Calculate_y(QPhiD,qs,dataX):
    ys = dataX@(QPhiD.T)
    return ys
```

We use a gaussian kernel for our implicit scalar valued kernel. We calculate the gram matrix between two (possibly different datasets $X \in \mathbb{R}^{d \times M}$, and $Y \in \mathbb{R}^{d \times N}$) with

```
def gaussianK(X,Y,sigma=kernSig):
    X2 = np.sum(X*X,axis=0)
    Y2 = np.sum(Y*Y,axis=0)
    XY = np.dot(X.T,Y)
    # -X2 - Y2 + 2XY = ||X-Y||^2
    # f(||X-Y||), f(np.sqrt(-X2 - Y2 + 2XY))
    return np.exp((-X2[:,None]-Y2[None,:]+2*XY)/(2*sigma**2))
```

M is then calculated using:

$$M = Q\Phi \cdot (G \cdot Q\Phi^T) \quad (339)$$

Where G is the gram matrix between two datasets $dataX$ and $dataY$. For M in the algorithm, $dataX = dataY$. It is interesting to note that in our algorithms we make heavy use of a connection between integration and matrix multiplication. This allows us to implement the integrations in a provably optimal way in terms of runtime.

```
# QPhi is the block diagonal matrix computed by the Calculate_QPhi function
def Calculate_M(QPhi,dataX,dataY,kernel=lambda X, Y : gaussianK(X,Y,sigma=
    kernSig)):
    G = kernel(dataX,dataY)
    return QPhi@(G@(QPhi.T))
```

Using properties of Kronecker products, we can solve the linear system in parallel by solving

$$(M + \lambda I)\alpha = Y^T \quad (340)$$

where $\alpha \in \mathbb{R}^{np \times d}$ We get this with the code:

```
# dataset - (dataX in  $\mathbb{R}^{d \times \sum\{i\} m_i}$ )
# ts      - (list of time vectors for dataset (could be different lengths)
#          )
# qs      - (list of time vectors of quadratures (could be different
#          lengths))
# n        - (number of features in the test space)
# lambdaReg - (Regularization term for the alpha)
# sigma    - (The scale parameter for the kernels)
# gaussianK - (A pointer to the implicit kernels)
def learn_alpha(dataset,ts,qs,n,lambdaReg=.0000001,sigma=kernSig,kern =
    gaussianK):
    Qphi, QphiD = Calculate_QPhi(qs,ts,n)
    M = Calculate_M(Qphi,dataset,dataset,kernel= lambda X, Y : kern(X,Y, sigma
    =sigma))
    ys = Calculate_y(QphiD,qs,dataset)
    alphas = np.linalg.solve(M+lambdaReg*np.eye(M.shape[0]),ys.T)
    return alphas, Qphi
```

We evaluate f at new datapoints with the almost the same code as we use to calculate M :

```
# Calculate f, requires Qhi, alpha, and the data to evaluate f at (dataX) as
# well as the data of the training set (dataY). (alpha should be matrix
# valued)
def Calculate_f(QPhi,dataX,dataY,alpha,kernel = gaussianK, sigma= kernSig):
    G = kernel(dataX,dataY,sigma)
    return alpha.T@((G@(QPhi.T)).T)
```

G.1 Legendre Polynomials

$$\sqrt{2} \quad T_0(x) = 1 \quad (341)$$

$$\sqrt{\frac{2}{3}} \quad T_1(x) = x \quad (342)$$

$$\sqrt{\frac{2}{5}} \quad T_2(x) = \frac{1}{2} (3x^2 - 1) \quad (343)$$

$$\sqrt{\frac{2}{7}} \quad T_3(x) = \frac{1}{2} (5x^3 - 3x) \quad (344)$$

$$\sqrt{\frac{2}{9}} \quad T_4(x) = \frac{1}{8} (35x^4 - 30x^2 + 3) \quad (345)$$

$$\sqrt{\frac{2}{11}} \quad T_5(x) = \frac{1}{8} (63x^5 - 70x^3 + 15x) \quad (346)$$

$$\vdots \quad \vdots \quad (347)$$

Where the term on the left denotes the $L^2([-1, 1])$ norm of the Legendre polynomial on the right.

References

- Jean-Luc Guermond Alexandre Ern. *Theory and Practice of Finite Elements*. Springer, 2004.
- Nicolas Boullé, Christopher J Earls, and Alex Townsend. Data-driven discovery of green’s functions with human-understandable deep learning. *Scientific reports*, 12(1):4824, 2022.
- Richard FitzHugh. Impulses and physiological states in theoretical models of nerve membrane. *Biophysical journal*, 1(6):445–466, 1961.
- Han Gao, Matthew J Zahr, and Jian-Xun Wang. Physics-informed graph neural galerkin networks: A unified framework for solving pde-governed forward and inverse problems. *Computer Methods in Applied Mechanics and Engineering*, 390:114502, 2022.
- Da Long, Nicole Mrvaljevic, Shandian Zhe, and Bamdad Hosseini. A kernel approach for pde discovery and operator learning, 2023. URL <https://arxiv.org/abs/2210.08140>.
- Edward N Lorenz. Deterministic nonperiodic flow. *Journal of atmospheric sciences*, 20(2): 130–141, 1963.
- E.N. Lorenz. Predictability: a problem partly solved. In *Seminar on Predictability*, volume 1, pages 1–18, Shinfield Park, Reading, 1995. ECMWF.
- Ha Quang Minh, Loris Bazzani, and Vittorio Murino. A unifying framework in vector-valued reproducing kernel hilbert spaces for manifold regularization and co-regularized multi-view learning. *Journal of Machine Learning Research*, 17(25):1–72, 2016.

- Houman Owhadi and Clint Scovel. *Operator-Adapted Wavelets, Fast Solvers, and Numerical Homogenization: From a Game Theoretic Approach to Numerical Approximation and Algorithm Design*, volume 35. Cambridge University Press, 2019.
- Vern I Paulsen and Mrinal Raghupathi. *An introduction to the theory of reproducing kernel Hilbert spaces*, volume 152. Cambridge university press, 2016.
- Maziar Raissi, Paris Perdikaris, and George E Karniadakis. Physics-informed neural networks: A deep learning framework for solving forward and inverse problems involving nonlinear partial differential equations. *Journal of Computational physics*, 378:686–707, 2019.
- Victor Rielly, Kamel Lahouel, Ethan Lew, Michael Wells, Vicky Haney, and Bruno Jedynak. Learning high-dimensional nonparametric differential equations via multivariate occupation kernel functions. *arXiv preprint arXiv:2306.10189*, 2023.
- Joel A. Rosenfeld, Rushikesh Kamalapurkar, Benjamin Russo, and Taylor T. Johnson. Occupation kernels and densely defined liouville operators for system identification. In *2019 IEEE 58th Conference on Decision and Control (CDC)*, pages 6455–6460, 2019. doi: 10.1109/CDC40024.2019.9029337.
- Joel A. Rosenfeld, Benjamin P. Russo, Rushikesh Kamalapurkar, and Taylor T. Johnson. The occupation kernel method for nonlinear system identification. *SIAM Journal on Control and Optimization*, 62(3):1643–1668, 2024. doi: 10.1137/19M127029X. URL <https://doi.org/10.1137/19M127029X>.
- Bernhard Schölkopf and Alexander J. Smola. *Learning with kernels : support vector machines, regularization, optimization, and beyond*. Adaptive computation and machine learning. MIT Press, 2002. URL <http://www.worldcat.org/oclc/48970254>.
- Robert Stephany and Christopher Earls. Pde-learn: Using deep learning to discover partial differential equations from noisy, limited data. *Neural Networks*, 174:106242, 2024.

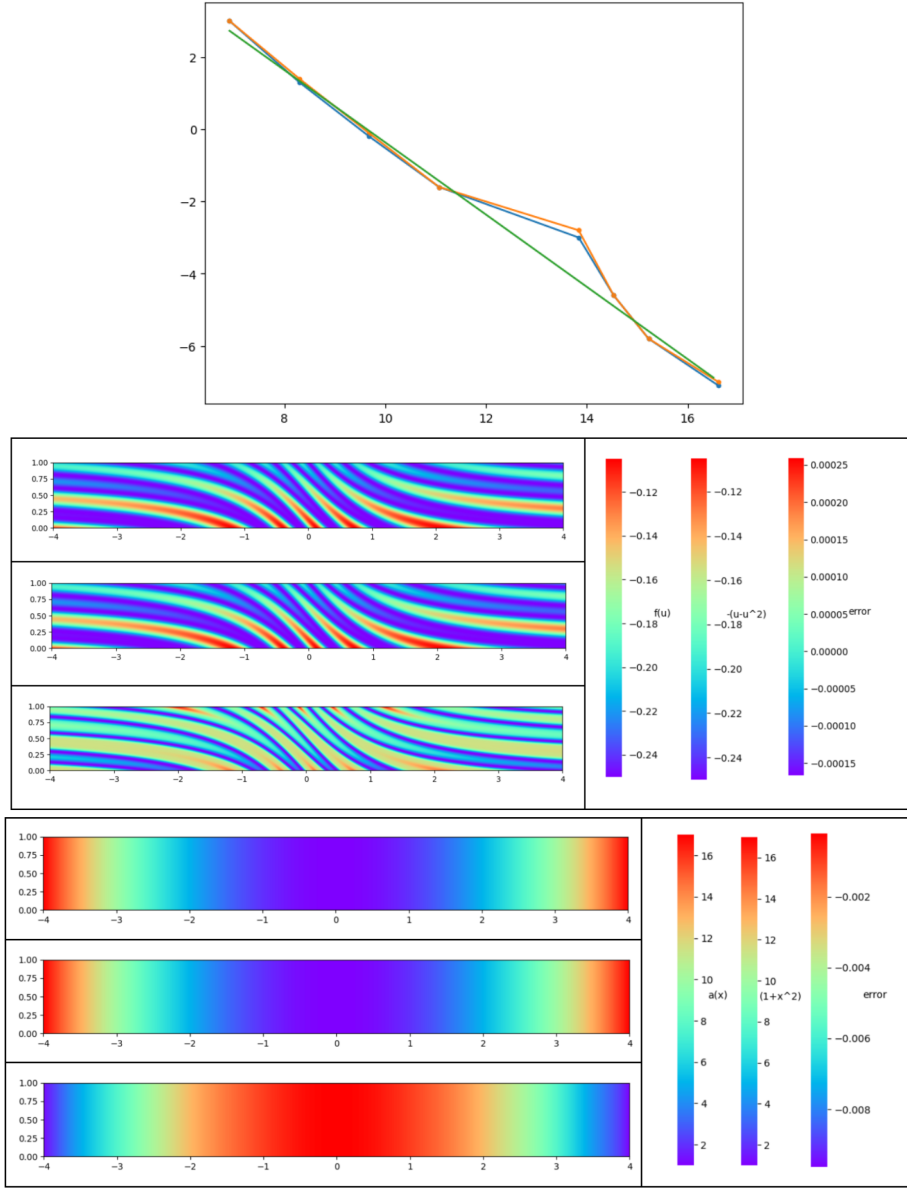


Figure 1: **Top:** Error of α in orange, and f in blue. A line with slope of negative one is plotted in green. The error is reported as $\|f' - f\|_1 / \|f\|_1$ where f' is the predicted function, f is the true function, and $\|\cdot\|_1$ is the l_1 norm. The errors, as a function of the number of observations are reported on a log-log scale. **Middle:** Prediction $f(u(x, y))$ over the $x y$ grid at the top, the ground truth in the middle, and the difference in the prediction and the ground truth is at the bottom. On the right, we present the scales for each of the three plots. **Bottom:** Prediction $\alpha(x)$ over the $x y$ grid at the top, the ground truth in the middle, and the difference between the prediction and the ground truth is at the bottom. On the right, we present the scales for each of the three plots.

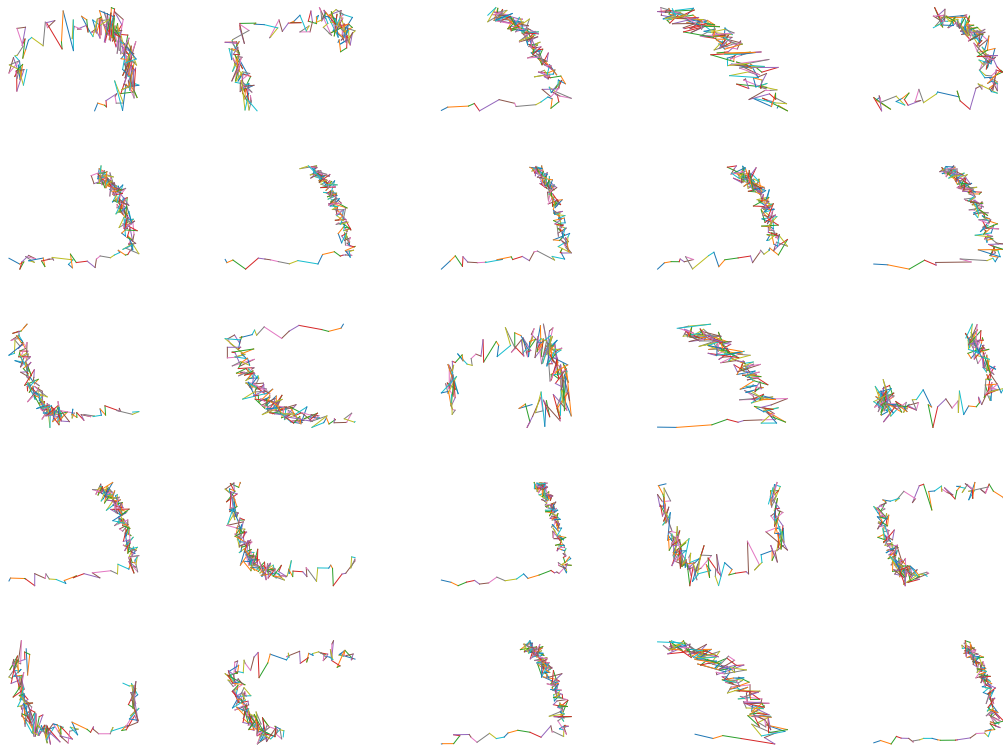


Figure 2: 25 randomly sampled trajectories in the NFHN (Noisy FHN) training set. Rielly et al. (2023)